Available online at www.sciencedirect.com
ScienceDirect
Bioorganic & Medicinal Chemistry
Bioorganic & Medicinal Chemistry 15 (2007) 6956–6974

Phenylethyl-substituted pyrimido[2,1-*f*]purinediones and related compounds: Structure–activity relationships as adenosine A_1 and A_{2A} receptor ligands

Anna Drabczyńska,[a] Christa E. Müller,[b] Anke Schiedel,[b] Britta Schumacher,[b] Janina Karolak-Wojciechowska,[c] Andrzej Fruziński,[c] Weronika Zobnina,[a] Olga Yuzlenko[a] and Katarzyna Kieć-Kononowicz[a,*]

[a]*Jagiellonian University Medical College, Faculty of Pharmacy, Department of Technology and Biotechnology of Drugs, Medyczna 9, Pl 30-688 Kraków, Poland*
[b]*Pharmaceutical Institute, University of Bonn, An der Immenburg 4, D-53121 Bonn, Germany*
[c]*Institute of General and Ecological Chemistry, Technical University of Łódź, Żwirki 36, Pl 30-924 Łódź, Poland*

Received 22 January 2007; revised 20 July 2007; accepted 27 July 2007
Available online 22 August 2007

Abstract—The synthesis of *N*-(un)substituted-phenylalkylpyrimido[2,1-*f*]purinediones was performed starting with 7-(3-chloropropyl)-8-bromotheophylline and 7-(3-chloropropyl)-8-bromo-1,3-dipropylxanthine. Compounds with unsubstituted or substituted ethylene spacer to an aromatic ring were synthesized. Additionally variations in the spacer—elongation of the linker containing more than two atoms, introduction of a double bond or heteroatoms were performed. Physicochemical properties of the synthesized compounds were described. The obtained compounds envisaged as sterically fixed and configurationally stable analogs of 8-styrylxanthines, were evaluated for their affinity to adenosine A_1 and A_{2A} receptors, the receptor subtypes that are predominant in the brain. Selected compounds were also investigated for the affinity to the A_{2B} and A_3 receptor subtypes. It was stated that phenylethyl pyrimido[2,1-*f*]purinediones and their analogs with variations of the ethylene spacer (substituted or extended) exhibit micromolar or submicromolar affinity for A_{2A} ARs (adenosine receptors); for example compound **2Ac** with *p*-hydroxy substituent displayed a K_i value of 0.23 μM at the rat A_{2A} receptor. In comparison to the previously obtained phenyl and benzyl pyrimido[2,1-*f*]purinediones compounds with a shorter spacer, phenethyl derivatives were optimal for A_{2A} AR. The kind of substituent at the aromatic ring was important for the affinity. Oxygen and nitrogen atoms in the spacer resulted frequently in a slight decrease of the A_{2A} AR affinity, introduction of more heteroatoms into the spacer—in carbamates—caused distinctly negative effect on the activity. In this series of compounds more frequently the adenosine A_1 activity was observed, also in submicromolar range as for dipropyl derivative **2Ba** with K_i value of 0.62 μM at the rat A_{2A} AR. 3D-QSAR models were developed for the compounds presented in this paper as well as in the previous publications showing activity at adenosine A_1 and A_{2A} ARs. It was concluded that for the activity at adenosine A_1 and A_{2A} receptors lipophilicity, steric effects along with the molecule's electrostatic surface properties had greatest value. Chosen compounds were evaluated in vivo as anticonvulsants in MES, scMet tests and examined for neurotoxicity. Contrary to previously obtained phenyl and benzyl pyrimido[2,1-*f*]purinediones, all tested compounds were inactive as anticonvulsants.

1. Introduction

Adenosine modulates a variety of important physiological processes and exhibits central nervous system depressant, cardiodepressant, antidiuretic, and immunomodulatory effects.[1] To date, four adenosine receptor subtypes: A_1, A_{2A}, A_{2B}, and A_3 have been cloned and pharmacologically characterized. These receptors belong to the superfamily of G-protein coupled receptors.[1,2] The A_1 and A_{2A} AR subtypes are high-affinity subtypes since they are usually activated by low, nanomolar concentrations of adenosine.[1,3] Adenosine A_1 receptors are widely distributed in the central nervous system and in peripheral tissues. The role of adenosine as neuroprotective agent during hypoxia and ischemic conditions seems to be mediated by the adenosine A_1 receptors. These receptors have been shown to be

Keywords: Adenosine A_1; A_{2A} receptor ligands; Pyrimido[2,1-*f*]purinediones; Tricyclic xanthine derivatives; Anticonvulsant activity.
* Corresponding author. Tel./fax: +48 12 657 04 88; e-mail: mfkonono@cyf-kr.edu.pl

0968-0896/$ - see front matter © 2007 Elsevier Ltd. All rights reserved.
doi:10.1016/j.bmc.2007.07.051

involved in sedative, antiseizure, and anxiolytic effects.[4] Selective A_1 antagonists may be useful as kidney-protective diuretics, for the treatment of congestive heart failure due to their diuretic and positive inotropic effects, and have potential for the treatment of brain diseases, such as depression or dementia.[5–8] The adenosine A_{2A} receptors play an important role in regulating smooth and well-coordinated movement in part by modulating the activity of dopamine-sensitive neurons. Adenosine A_{2A} receptors are located in brain primarily in the striatum where they are colocalized with dopamine D_2 receptors. There is now accumulating evidence that adenosine A_{2A} receptor antagonists may provide a novel therapy for the treatment of Parkinson's disease with lower risk of dyskinesias and may exhibit neuroprotective effects.[8–10]

In our efforts to develop new ligands for A_1 and A_{2A} adenosine receptors, oxygen- or nitrogen-containing annelated theophylline derivatives with the following (**I**, **II**) structures (Table 1) were obtained.[11–16]

Selective adenosine A_{2A} receptor antagonists were identified especially among the series of pyrimido[2,1-*f*]purinediones (**IIa**, **IIb**). Replacement of dimethyl ($R^4 = CH_3$) with dipropyl substituents in the purine ring improved the affinity to A_1, A_{2A}, and A_3 ARs and therefore reduced A_{2A}-selectivity (**IId**, **IIc**, **IIg**). Derivatives with good adenosine A_1 receptor affinity (**Ib**, **IId**, **IIf**, and **IIg**) were identified as well[15,16] (Table 1).

As a continuation of our research, pyrimido[2,1-*f*]purinediones of the general structure **III** connected by an unsubstituted or substituted ethylene spacer to an aromatic ring (lead compound: 1,3-dimethyl-9-phenethylpyrimido[2,1-*f*]purine **2Aa**) were synthesized (Fig. 1). In order to investigate structure–activity relationships

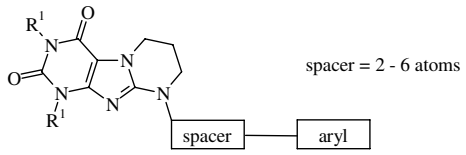

III

Figure 1. General structure of the obtained pyrimido[2,1-*f*] purinediones.

(SARs) of the new series of compounds, variations in the spacer (elongation of the linker containing more than two atoms, introduction of a double bond or heteroatoms) were performed. 1,3-Dipropyl-substituted structures (R^1 = propyl) were compared with dimethyl derivatives (R^1 = Me).

2. Chemistry

The synthesis of the target compounds was performed as depicted in Figure 2. The synthesis of *N*-phenylalkylpyrimido[2,1-*f*]purinediones was accomplished as shown in Figure 2a. As starting materials 7-(3-chloropropyl)-8-bromotheophylline (**1A**) and 7-(3-chloropropyl)-8-bromo-1,3-dipropylxanthine (**1B**) were used, which could be obtained as previously described by us.[15–17] They were cyclisized with phenylalkylamines under various reaction conditions regarding the amount of amine, the reaction medium, and the reaction time (see Table 2a). Two amines, 4-hydroxyphenylethylamine (tyramine) and 2-amino-1-phenyl-1-propanol (norephedrine), were obtained from their hydrochlorides by alkalization of water solutions of their hydrochlorides to pH 9 by 10% aqueous sodium carbonate (tyramine), or 15% aqueous sodium hydroxide (norephedrine). Acetyl derivatives **2Ag** and **2Ah** were prepared by

Table 1. Oxygen- or nitrogen-containing annelated theophylline analogs. Adenosine A_1/A_{2A} receptors affinity of chosen tricyclic annelated theophylline derivatives of type **I** and **II**[12–16] in comparison with the standard compounds caffeine and KW-6002

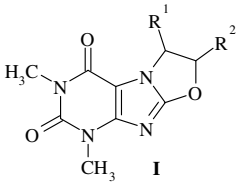

I

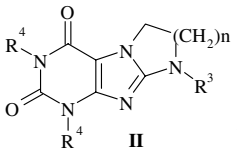

II n= 1, 2, 3

Compound	R^1	R^2	R^3	R^4	A_1 K_i ± SEM (μM) versus [^{3}H]CCPA	A_{2A} K_i ± SEM (μM) versus [^{3}H]MSX-2
Ia	H	Octyl	—	—	>25	0.998 ± 0.05
Ib	H	$C_6H_5CH_2$	—	—	2.07 ± 0.15	8.39 ± 1.76
Ic	H	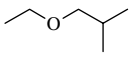	—	—	>25	2.67 ± 0.54
IIa	—	—	2-Naphtyl	CH_3	>25	0.219 ± 0.007
IIb	—	—	4-F-C_6H_4	CH_3	>25	0.147 ± 0.02
IIc	—	—	2-Naphtyl	$CH_3CH_2CH_2$	1.285 ± 0.32	0.398 ± 0.111
IId	—	—	4-Cl-C_6H_4	$CH_3CH_2CH_2$	0.36 ± 0.06	0.376 ± 0.095
IIe	—	—	2-$OCH_3C_6H_4CH_2$	CH_3	>25	0.699 ± 0.016
IIf	—	—	3-$ClC_6H_4CH_2$	$CH_3CH_2CH_2$	0.089 ± 0.029	1.29 ± 0.31
IIg	—	—	4-$ClC_6H_4CH_2$	$CH_3CH_2CH_2$	0.23 ± 0.15	0.87 ± 0.41
Caffeine					18.8 ± 5.6	32.5 ± 8.0
KW-6002					0.230 ± 0.030	0.00515 ± 0.00025

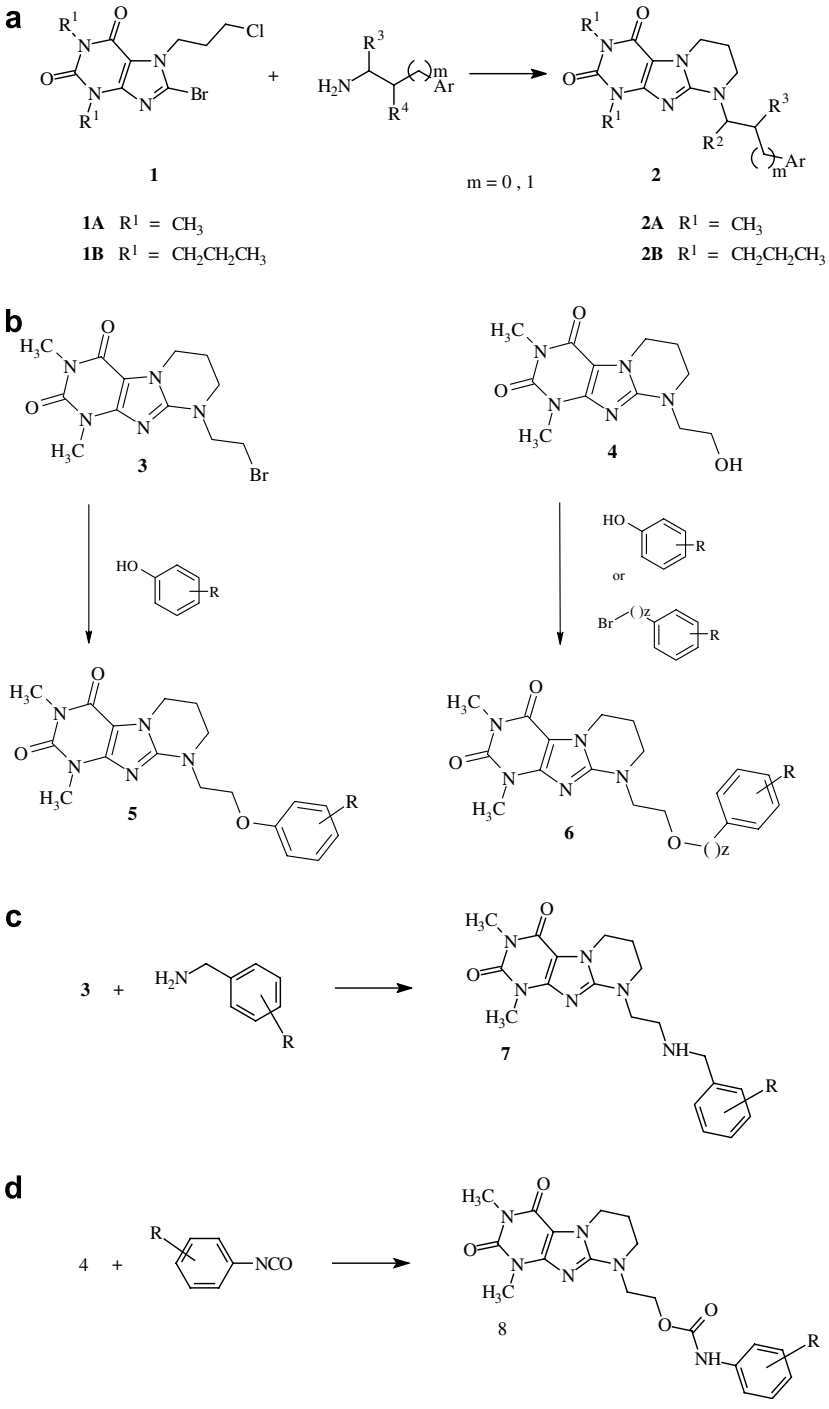

Figure 2. Synthesis of the pyrimido[2,1-*f*]purinediones containing spacer between tricyclic skeleton and (un)substituted aromatic ring. (a) Spacer-consisting of carbon (un)branched chain. (b) Spacer-containing one heteroatom (oxygen). (c) Spacer-containing one heteroatom (nitrogen). (d) Spacer-containing more heteroatoms. Some products (**7**) were obtained under microwave irradiation.

acetylation of the hydroxyl compounds **2Ae** and **2Af** with acetic anhydride.

The compound **5a** with a phenoxyalkyl moiety (Fig. 2b) was obtained by Williamson's reaction of 9-bromoethyl-1,3-dimethyl-6,7-dihydro-6,7,8,9-tetrahydropyrimido[2,1-*f*]purine-2,4(1*H*,3*H*)dione (**3**)[18] with sodium salt of *p*-chlorophenol (prepared ex tempore from *p*-chlorophenol) (Table 2b, method C).

The compounds **5b** and **5d** were obtained by the reaction of **3** with the appropriate sodium phenolate (generated with sodium hydride from the phenol) in acetonitrile using [15]-crown-5 as a phase-transfer catalyst (Table 2b, method A). Similar reaction conditions were used for the synthesis of the compounds **6a**–**6d**. The ethers were obtained starting from 1,3-dimethyl-9-hydroxyethyl-6,7-dihydro-6,7,8,9-tetrahydropyrimido[2,1-*f*]purine-2,4(1*H*,3*H*)dione (**4**),[19] transformed with sodium

Table 2a. Reaction conditions and physicochemical properties of the phenylalkylpyrimido [2,1-*f*]purinediones

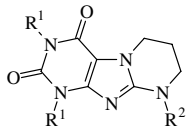

Compound	R^1	R^2	Mp (°C)	Yield (%)	Reaction medium excess of amine	Reaction time (h)	Crystallization solvent	TLC R_f
2Aa	CH_3	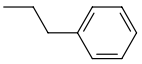	195–197	58	Propanol, 1.6	5	50% Ethanol	0.64 (1)[a]
2Ab	CH_3	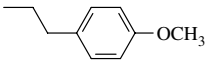	203–206	88	Propanol, 2	5	Butanol	0.45 (1)
2Ac	CH_3	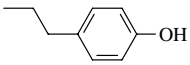	175–178	85	Methoxyethanol, 2	10	Ethanol	0.34 (1)
2Ad	CH_3	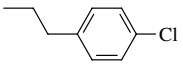	233–235	90	—, 7	5	Butanol	0.45 (1)
2Ae	CH_3	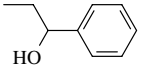	199–202	80	Methoxyethanol, 2	10	Ethanol	0.45 (1)
2Af	CH_3	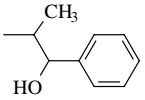	216–218	67	Methoxyethanol, 2	10	Methoxyethanol	0.44 (1)
2Ag	CH_3	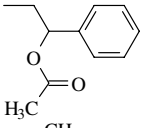	191–193	98	Acetic anhydride, 25 [b]	5	Propanol	0.56 (1)
2Ah	CH_3	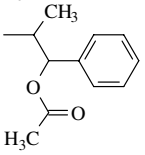	234–235	94	Acetic anhydride, 25 [b]	5	Methoxyethanol	0.36 (1)
2Ai	CH_3	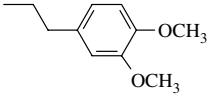	164–166	91	Propanol, 2	5	Isopropanol	0.31 (1)
2Aj	CH_3	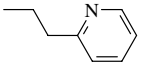	175–177	76	Butanol, 2	6	Isopropanol	0.10 (1)
2Ak	CH_3	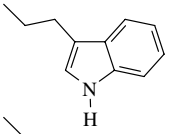	230–232	53	Methoxyethanol, 2	10	Propanol	0.51 (1)
2Al	CH_3	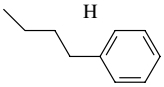	159–161	53	Propanol, 1.4	10	50% Ethanol	0.70 (1)
2Bb		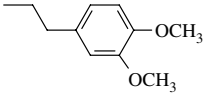	124–125	83	DMF, 3	5	Ethanol/H_2O	0.57 (1)
2Ba		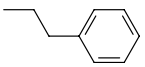	125–126	90	DMF, 5	5	Ethanol/H_2O	0.66 (1)
2Bc		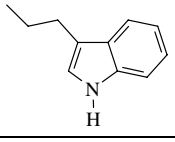	164–166	96	Methoxyethanol, 2	10	Propanol	0.65 (1)

[a] Developing system (1).
[b] Excess of acetic acid anhydride.

Table 2b. Reaction conditions and physicochemical properties of the derivatives containing heteroatoms in the spacer connecting tricyclic skeleton with (un)substituted aromatic ring

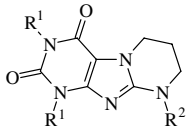

Compound	R^1	R^2	Mp (°C)	Method yield (%)	Reaction time (h)	Crystallization solvent	TLC R_f
5a	CH_3	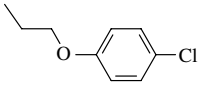	146–148	C (46)	20	EtOH	0.47 (1)
5b	CH_3	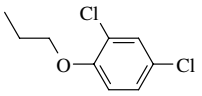	155–158	A (33)	5.5	50% EtOH	0.29 (2)
5c	CH_3	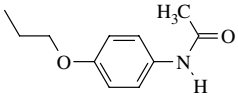	192–193	B (18)	6	50% EtOH	0.15 (3)
5d	CH_3	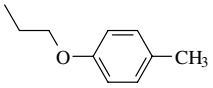	149–151	A (10) B (48)	6	AcOEt/$CHCl_3$ (1:1)	0.40 (2)[a]
6a	CH_3	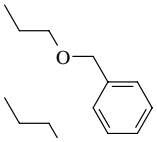	132–135	D (19)	6	50% EtOH	0.27 (3)
6b	CH_3	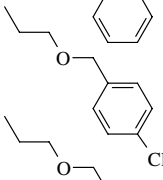	107–110	D (25)	6	50% EtOH	0.16 (2)
6c	CH_3	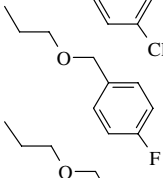	104–106	D (16)	6	50% EtOH	0.21 (2)
6d	CH_3	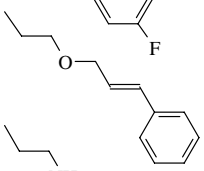	158–160	D (16)	7	50% EtOH	0.19 (2)
7a	CH_3	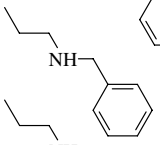	280–285	E (22)		EtOH	0.30 (4)
7b	CH_3	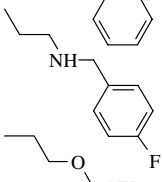	156–159	E (13)		EtOH	0.32 (4)
8a	CH_3	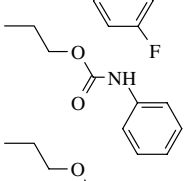	234–236	F (78)	10	EtOH	0.64 (5)
8b	CH_3	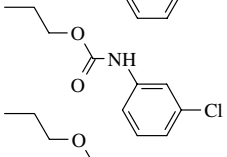	250–252	F (70)	12.5	EtOH	0.64 (5)
8c	CH_3	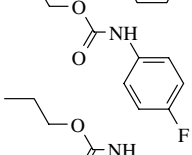	262–266	F (67)	10	EtOH	0.60 (5)
8d	CH_3	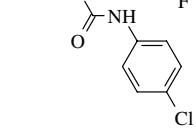	264–266	F (67)	11		0.62 (5)

[a] Developing system (1)–(4) or (5).

hydride to the required ethanolate, and reacted with the appropriate (un)substituted benzyl chlorides or bromides in dry toluene in the presence of [15]-crown-5 as a catalyst (Table 2b, method D). For compounds **5c** and **5d**, a Mitsunobu reaction protocol was also used starting with (**4**) and the appropriate phenol derivative.[20] The amines **7a** and **7b** (Fig. 2c) were obtained as products of the reaction of **3** and appropriate (un)substituted benzylamines by melting the reagents upon microwave irradiation under solvent-free conditions[21,22] (Table 2b, method E). The reaction of **4** and (un)substituted phenyl isocyanates (Fig. 2d), carried out in acetonitrile, yielded the carbamates **8a**–**8d** (Table 2b, method F).

The reaction conditions and physicochemical properties of the obtained compounds are summarized in Tables 2a and 2b.

The structures of the synthesized compounds were confirmed by elemental analyses, as well as UV, IR and ^{1}H NMR spectral analysis. In UV spectra of pyrimido[2,1-*f*]purinediones, a bathochromic shift of λ_{max} from ca 275 nm to about 300 nm, typical for 8-aminoxanthine derivatives, was observed.[23] Examined compounds showed IR absorption bands typical for xanthine derivatives[24] and in ^{1}H NMR adequate shifts could be observed.

3. X-ray structure analysis of compound 6d

In all derivatives described in this paper, flexible chain (spacer) joins main molecule skeleton and aromatic ring. These spacers may be classified as aliphatic or heteroaliphatic ones. In the aliphatic (or heteroaliphatic) chain, theoretically, each bond possesses rotational freedom and the number of possible low energy conformations depends on the number and nature of the atoms. For that reason, from the structural viewpoint, the spacer seemed to be a particularly interesting element of the studied species. Having that in mind, it was decided to study the structure of the molecule **6d** with the most complex and the longest spacer. Basing on that structure, after small modifications all remaining molecules can be roughly constructed and used as a starting point for geometry optimization.

The compound **6d** consists of the main tricyclic ring system and aromatic substituent joined to the core of the molecule via long (—CH_2—CH_2—O—CH_2—CH=CH—) spacer at N9 atom (Fig. 3). The atoms C6, C7, and C8 from the six-membered pyrimidine ring and the atoms of C14—C16=C17—Ph from the flexible chain—in the crystal—are disordered with structure occupation factors (s.o.f.s) equal to 0.42 and 0.62, respectively, for both parts mentioned above. Although the parts of disordered spacer exhibit the opposite signs of the torsion angles value, the molecule adopts an extended conformation (Fig. 3). The undulated six-membered pyrimidine ring adopts a half-chair conformation. In both disordered residues, C7 atom is in flap position and is located above or below the main ring plane defined by the remaining ring atoms in the two disordered species. In the crystal, the molecules are joined in dimmers with the weak H-bond of C6—H6B...O4 (3.319 Å).

4. Pharmacology

All compounds were tested in vitro in radioligand binding assays for the affinity to A_1 and A_{2A} adenosine receptors of the rat brain cortical membrane (A_1), and the rat brain striatal membrane (A_{2A}) preparations. Some selected compounds were further tested for their affinity to the human recombinant adenosine A_1, A_{2A}, A_{2B}, and A_3 receptors stably expressed in Chinese hamster ovary (CHO). The following radioligands were used: [^{3}H]2-chloro-N^6-cyclopentyladenosine ([^{3}H]CCPA) for A_1, [^{3}H]1-propargyl-3-(3-hydroxypropyl)-7-methyl-8(*m*-methoxystyryl)xanthine ([^{3}H]MSX-2)[25,26] for A_{2A}, [^{3}H]4-(2-[7-amino-2-(2-furyl)-[1,2,4]-triazolo[2,3-*a*]-1,3,5-triazin-5,4-(amino)-ethyl)-phenol ([^{3}H]ZM241385)[27] or [^{3}H]8-((4-(2-hydroxyethylamino)2-oxo-ethoxy)phenyl)-1-propylxanthine [^{3}H]PSB-298[28,29] for A_{2B}, and [^{3}H]2-phenyl-8-ethyl-4-methyl-(8*R*)-4,5,7,8-tetrahydro-1*H*-imidazo[2,1-*i*]purine-5-one ([^{3}H]PSB-11)[30] for A_3 binding studies.

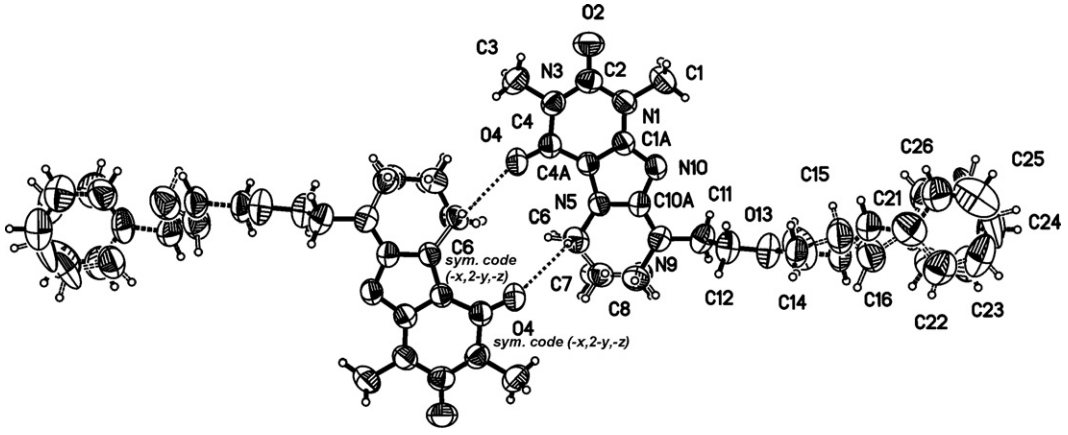

Figure 3. Molecules of **6d** joined in dimmer by O4...H6b–C6 weak H-bonds. Disordered atoms (C6, C7, and C8) and disordered substituent at N9 atom are depicted.

Based on our former observations that tricyclic purinediones can possess anticonvulsant activity,[12–14] the compounds **2Aa**–**2Al**, **5a**–**d**, and **8a**–**d** were also evaluated in vivo as potential anticonvulsants by the ADD (Antiepileptic Drug Development) Program of the National Institute of Neurological Disorders and Stroke (NINDS) according to ASP (Antiepileptic Screening Project) protocols. Compounds were injected intraperitoneally as a suspension in 0.5% methylcellulose into the mice and evaluated in the preliminary screenings with at least three dose levels (30, 100, and 300 mg/kg at 0.5 and 4 h time periods). Phase I of the evaluation included three tests: maximal electroshock (MES), subcutaneous pentylenetetrazole (scMet) seizure tests, and the rotorod test for neurological toxicity (Tox). The tests were described in detail by Stables and Kupferberg.[31–33]

The MES assay is a model for generalized tonic–clonic seizures, it identifies these compounds which prevent seizure spread and has predictive value for the agents of therapeutic potential in the management of grand mal epilepsy. The scMet test is a model that primarily identifies compounds that raise seizure threshold; these compounds are likely to be effective against petit mal. For some compounds, namely **5b**, **5d**, and **8d**, the mice 6-Hz test was performed at dose 100 mg/kg. A mice 6 Hz screening is an alternative electroshock model in which a 6-Hz electrical stimulus is administered for a prolonged period. The 6-Hz model appears to be sensitive to a different spectrum of anticonvulsants than in the MES test and may detect agents that are ineffective in the standard anticonvulsant screening models.[34,35]

5. Biological results

5.1. In vitro tests: structure–activity relationships

The results of the radioligand binding assays at the adenosine receptors are presented in Table 3a for the compounds with a (un)branched carbon chain as a spacer, in Table 3b for dipropyl derivatives, and in Table 3c for the compounds with spacers containing heteroatoms.

The results in the group of arylalkyl derivatives showed compounds with preferably and the most expressed affinity for the rat adenosine A_{2A} receptors. Elongation

Table 3a. Adenosine receptors affinities of the pyrimido[2,1-*f*]purinediones with (un)substituted alkyl spacer between tricyclic ring system and aromatic substituent

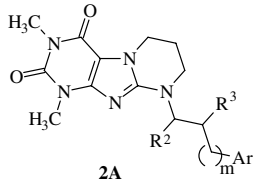

2A

Compound	*m*	R^2	R^3	Ar	$K_i \pm$ SEM (μM)			
					Rat A_1 (human A_1)	Rat A_{2A} (human A_{2A})	Human A_{2B}	Human A_3
Caffeine					18.8 ± 5.6[a]	32.5 ± 8.0[a]		
KW-6002					0.23 ± 0.03[a]	0.00515 ± 0.00025[a]		
2Aa	0	H	H	C_6H_5	>25 (31%)[a] (>10 (44%))[a]	0.32 ± 0.03[a] (2.89 ± 0.75)[a]	ca. 10 (57%)[b,c]	>10 (20%)[b]
2Ab	0	H	H	4-$OCH_3C_6H_4$	3.85 ± 0.43[a]	0.37 ± 0.02[a]	nd	nd
2Ac	0	H	H	4-OHC_6H_4	ca. 25 (46%)[a] (⩾25 (34%))[a]	0.23 ± 0.01[a] (0.63 ± 0.35)[a]	7.20 ± 0.60[b,c]	>10 (9%)[b]
2Ad	0	H	H	4-ClC_6H_4	6.47 ± 1.15[a]	0.48 ± 0.11[a]	nd	nd
2Ae	0	H	OH	C_6H_5	ca. 25 (49%)[a]	1.11 ± 0.26[a]	nd	nd
2Af	0	CH_3	OH	C_6H_5	ca. 25 (45%)[a]	2.16 ± 0.11[a]	nd	nd
2Ag	0	CH_3	$OCOCH_3$	C_6H_5	3.40 ± 0.64[a]	1.22 ± 0.45[a]	nd	nd
2Ah	0	H	$OCOCH_3$	C_6H_5	ca. 25 (50%)[a]	1.00 ± 0.38[a]	nd	nd
2Ai	0	H	H	3,4-di-$OCH_3C_6H_3$	⩾25 (33%)[a]	1.21 ± 0.19[a]	nd	nd
2Aj	0	H	H		>25 (22%)[a]	>25 (37%)[a]	13.4 ± 4.7[b,c]	≫10 (0%)[b]
2Ak	0	H	H	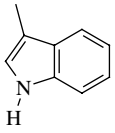	ca. 25 (41%)[a] (>25 (21%))[a]	0.33 ± 0.07[a] (4.56 ± 0.81)[a]	ca. 10 (56%)[b,c]	>10 (21%)[b]
2Al	1	H	H	C_6H_5	1.99 ± 0.46[a]	1.10 ± 0.14[a]	nd	nd

nd, not determined.
[a] Tested at 25 μM.
[b] Tested at 10 μM.
[c] Tested versus [^{3}H]ZM-241385.

Table 3b. Adenosine receptors affinities of the dipropyl-substituted pyrimido[2,1-*f*]purinedione derivatives (**2B**)

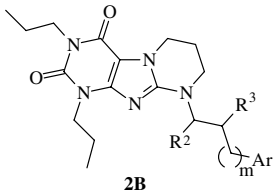

2B

Compound	*m*	R^2	R^3	Ar	$K_i \pm$ SEM (μM)			
					Rat A_1	Rat A_{2A}	Human A_{2B}	Human A_3
Caffeine					18.8 ± 5.6[a]	32.5 ± 8.0[a]		
KW-6002					0.23 ± 0.03[a]	0.00515 ± 0.00025[a]		
2Ba	0	H	H	C_6H_5	0.62 ± 0.22[a]	0.86 ± 0.09[a]	0.59 ± 0.06[b,d]	3.66 ± 0.77[c]
2Bb	0	H	H	3,4-di-$OCH_3C_6H_3$	0.82 ± 0.20[a]	1.33 ± 0.12[a]	nd	≫1 (3%)[c]
2Bc	0	H	H	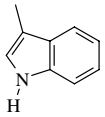	1.79 ± 0.48[b]	0.90 ± 0.11[b]	nd	≫1 (9%)[c]

nd, not determined.
[a] Tested at 25 μM.
[b] Tested at 10 μM.
[c] Tested at 1 μM.
[d] Tested versus [^{3}H]ZM-241385.

of the spacer from ethyl (**2Aa**) to propyl one (**2Al**) caused almost 3-fold reduction of A_{2A} potency (K_i A_{2A} values of 0.32 ± 0.03 μM and 1.10 ± 0.14 μM, respectively). It seems that the spacer containing two carbon atoms is an optimal one because the previously described phenyl[15] and benzyl[16] pyrimido[2,1-*f*]purinediones have shown worse K_i A_{2A} values of ⩾25 μM and 1.09 ± 0.30 μM, respectively. That sequence of K_i A_{2A} values brings to a supposition that the activity is able to correlate with the mutual positions of phenyl rings and pyrimido[2,1-f]purinedione skeletons in the species possessing –$(CH_2)_n$– spacer, where *n* = 0, 1, 2, or 3 carbon atoms, respectively. To describe qualitatively those geometrical spacer phenomena, parameter marked as *Δ* (Å) waspproposed. That parameter defines "out of plane" position for the first atom of phenyl ring with respect to the main plane of the molecule (Fig. 4a). Based on our previous[15,16] and current crystallographic studies, the rough models of four pyrimido[2,1-*f*]purinediones were built and optimized at semi-empirical quantum chemistry level. Then it was found that *Δ* parameters equal to 0.55, 1.86, 2.50, and 3.46 Å for molecules with –$(CH_2)_n$–spacer encompassing 0, 1, 2, or 3 carbon atoms, respectively. Obtained *Δ* values correlate well with the compounds' activity to A_{2A} receptor (Fig. 4b). Due to parabolic relation, minimum of K_i A_{2A} is observed for *n* = 2, that is for ethyl (**2Aa**) derivative.

Exchange of the phenyl ring to a 2-pyridyl one (**2Aj**) is not accepted, while for 3-indolyl substituent (**2Ak**) activity remains almost unchanged. Introduction of one substituent into the phenyl ring is allowed; it may be beneficial as it is observed with 4-OH (**2Ac**), or causes slight decrease of the activity (**2Ab**, **2Ad**); two substituents: 3,4-di-OCH_3 (**2Ai**) decreased 4-fold the A_{2A} activity. Introduction of the substituents into the spacer was disadvantageous for the A_{2A} activity (**2Ae**–**2Ah**).

In this group of compounds, only four structures (**2Al**, **2Ag**, **2Ab**, and **2Ad**—ordered in decreasing activity) exhibited low micromolar activity toward the rat adenosine A_1 receptor. In the series of dipropyl derivatives (**2Ba**–**2Bc**) (see Table 3b), slightly lower A_{2A} activity was maintained accompanied with beneficial activity toward adenosine A_1 receptors. This tendency was also noticed for the previously described phenyl[15] and benzyl[16] pyrimido[2,1-*f*]purinediones. Additionally, similar to the dimethyl derivatives with ethyl spacer, in the series of dipropyl derivatives, the influence of 3-indolyl substituent (**2Bc**) and double substituent in phenyl ring (**2Bb**) caused analogous adenosine A_{2A} receptors effects.

In the series of ether derivatives containing one heteroatom—oxygen in the spacer (**5a**–**5d** and **6a**–**6d**) (see Table 3c)—similar, low micromolar adenosine A_{2A} activity was observed, slightly dependent on the kind (one substituent—**5a**, **5c**, **5d**, **6b**, and **6c**) and the number of substituents (two substituents—**5b**) in the phenyl ring. As well, length of the spacer had small, rather disadvantageous influence on the adenosine A_{2A} activity (cf. **5c**, **6c**, and **6d**). In this series of compounds more frequently the adenosine A_1 activity was observed, almost equal activity toward these two ARs subtypes was noticed as well (**6a** and **6c**). Compounds containing one heteroatom—nitrogen in the spacer (**7a** and **7b**) (see Table 3c)—have shown micromolar activity towards adenosine A_1 and A_{2A} receptors, better than the former mentioned.

Introduction of more heteroatoms into the spacer—carbamates **8a** –**d** (Table 3c)—had distinctly negative influence on the adenosine A_1 and A_{2A} receptors affinity.

Summing up, the best A_{2A} ARs ligands were compounds **2Ac** > **2Aa** > **2Ak** > **2Ab** from the phenyl ethyl

Table 3c. Adenosine receptors affinities of the pyrimido[2,1-*f*]purinediones with the spacers containing heteroatoms

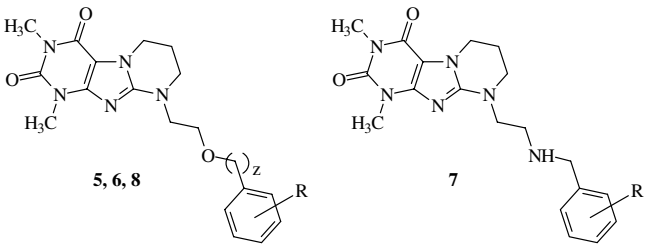

Compound	*z*	R	$K_i \pm$ SEM (μM)			
			Rat A_1	Rat A_{2A}	Human A_{2B}	Human A_3
Caffeine			18.8 ± 5.6[a]	32.5 ± 8.0[a]		
KW-6002			0.23 ± 0.03[a]	0.00515 ± 0.00025[a]		
(1) One heteroatom—oxygen						
5a	—	4-Cl	4.22 ± 0.53[a]	ca. 25 (49%)[a]	ca. 10 (44%)[b,e]	ca. 10 (45%)[b]
5b	—	2,4-di-Cl	3.50 ± 0.72[b]	1.09 ± 0.21[b]	nd	≫1 (0%)[c]
5c	—	4-$NHCOCH_3$	ca. 10 (41%)[b]	2.02 ± 0.81[b]	nd	≫1 (0%)[c]
5d	—	4-CH_3	ca. 10 (41%)[b]	4.60 ± 1.53[b]	nd	≫1 (2%)[c]
6a	1	H	3.16 ± 0.76[b]	3.69 ± 0.39[b]	nd	≫1 (0%)[c]
6b	1	4-Cl	ca. 10 (48%)[b]	1.33 ± 0.24[b]	nd	nd
6c	1	4-F	3.68 ± 0.98[b]	3.05 ± 0.24[b]	nd	≫1 (0%)[c]
6d	$CH_2CH{=}CH$	H	ca. 10 (36%)[b]	4.29 ± 1.20[b]	nd	≫1 (0%)[c]
(2) One heteroatom—nitrogen						
7a	—	H	7.55 ± 2.35[b]	20.0 ± 2.0[b]	>10 (27%)[b,d]	nd
7b	—	4-F	2.63 ± 0.21[b]	14.0 ± 1.5[b]	nd	nd
(3) More heteroatoms						
8a	C(O)NH	H	≫10 (3%)[b]	>10 (35%)[b]	nd	nd
8b	C(O)NH	3-Cl	>10 (10%)[b]	>10 (33%)[b]	nd	nd
8c	C(O)NH	4-F	>10 (13%)[b]	⩾ 10 (42%)[b]	nd	nd
8d	C(O)NH	4-Cl	>10 (24%)[b]	>10 (32%)[b]	nd	nd

nd, not determined.
[a] Tested at 25 μM.
[b] Tested at 10 μM.
[c] Tested at 1 μM.
[d] Tested versus [^{3}H]PSB-298.[26,27]
[e] Tested versus [^{3}H]ZM-241385.

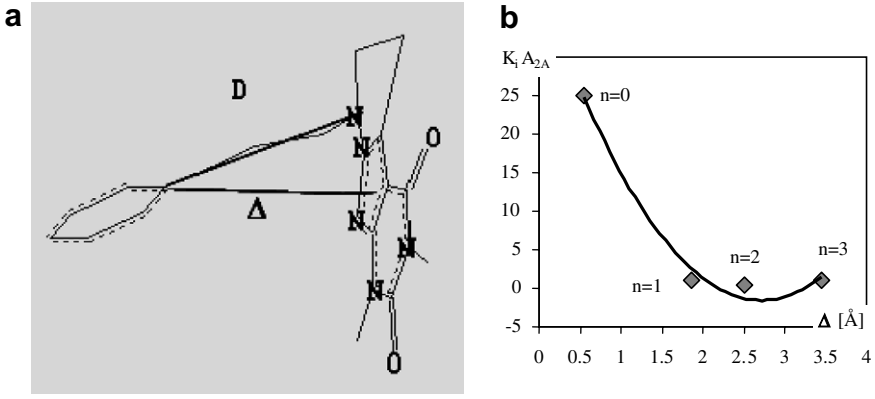

Figure 4. (a) Illustration for the parameter *Δ* (Å) defining mutual positions of the phenyl rings with respect to pyrimido[2,1-*f*]purinedione skeleton. (b) Relationship between K_i and A_{2A} potency of pyrimido[2,1-*f*]purinediones with phenyl substituent separated by $(CH_2)_n$ aliphatic spacer.

series and the best A_1 AR affinity was shown by the dipropyl derivatives **2Ba > 2Bb > 2Bc > 2Al > 7b** (phenylpropyl derivative and one from amines).

Compounds **2Aa**, **2Ac**, and **2Ak** were additionally tested at the human adenosine A_1 and A_{2A} receptors. The activity at A_1 receptors was less influenced than at A_{2A}

receptors. Here, the less pronounced activity was observed in the range of 3-fold (**2Ac**) to ca. 10-fold or more (**2aA** and **2Ak**).

In Tables 3a–3c, the results of the binding assays toward human adenosine A_{2B} and A_3 receptors for chosen compounds are presented. Dipropyl derivative **2Ba** has shown submicromolar affinity for adenosine A_{2B} receptor, less active were **2Ac**, **2Aa**, **2Ak**, and **2Aj**. All compounds were those with two carbon atoms spacer.

No remarkable affinity to adenosine A_3 receptor was found for the investigated compounds **2Aa**, **2Ac**, **2Aj**, **2Ak**, **2Bb**, **2Bc**, **5a–d**, **6a**, **6c**, **6d** (only dipropyl derivative **2Ba** has shown low micromolar activity).

In our previous work[15], it was stated that tricyclic purinediones act as antagonists at adenosine A_{2A} receptors in the result of their functional properties evaluation using a sodium chloride shift assay.[36] Considering the similarity in the structures of the new examined compounds, it may be supposed that they also act as antagonists at adenosine A_{2A} receptors.

5.2. In vitro tests: quantitative structure–activity relationships

3D-QSAR analyses were performed for the compounds which showed activity at adenosine A_1 and adenosine A_{2A} receptors. Topological, geometric, and electronic descriptors were calculated by means of the program CAChe 6.1.1.[37] Because of the small database, we used the whole sample for the calibration and checked the fit by cross-validation[38] instead of holdout data set.[39,40]

Determination of the linear equation that best represented the dependence of the A_1 and A_{2A} AR binding affinity on several input descriptors was carried out using MLR (multiple linear regression) technique. The statistical parameters used for the model development and validation are as follows: R^2 is the correlation coefficient, q^2 is the leave-one-out cross-validated R^2, k and k' are the slopes of the regression predicted affinity versus observed and observed affinity versus predicted,[39,40] F is the test F value. The algorithm we used to select the best descriptors and models is summarized below.

1. The correlation equations with $1, 2, \ldots,$ NDmax descriptors (maximum number of descriptors equals 5) were calculated using ProjectLeader CAChe 6.1.1[37]application. The ratio of the number of compounds and number of variables is at least 5:1.[41]
2. An exclusion of the descriptor in any pair of descriptors whose pairwise correlation exceeds 0.85 was carried out.[38,42,43]
3. The single linear regressions were calculated to choose the descriptors with the best correlation to ligands' affinity. Two parameters linear regressions were determined to choose best pairs of the descriptors for predicting ligands' affinity. The same procedure was applied for the triple linear regression.
4. The next one descriptor was added and multiple linear regression analysis was performed.
5. If the regression parameters q^2 and R^2 for ND = 4 were lower than for ND = 3, then stepped up to 4. If the regression parameters q^2 and R^2 for ND = 4 were higher than for ND = 3, then the equation was stored. The same procedure was applied up to ND = NDmax.
6. The equations having the highest q^2 and R^2 were collected and k, k', and F were calculated.
7. The equation with the best statistical parameters was chosen.

3D-QSAR analyses were performed for the compounds as well presently as previously described,[15,16] which showed activity at adenosine A_1 and adenosine A_{2A} receptors.

5.2.1. A_1 AR QSAR. For the development of A_1 AR 3D-QSAR model, 31 ligands (**9**, **10**, **16**, **21**, **29**, **39**, **40**;[15] **1**, **5**, **10**, **13–20**;[16] **2Ab**, **2Ad**, **2Ag**, **2Al**, **2Ba–c**, **5a**, **b**, **6a**, **6c**, **7a**, and **7b**) were used. The model selected as the best one included the smallest number of descriptors together with the largest values of q^2 and R^2. The following 3D-QSAR Eq. 1 that best predicts the A_1AR ligands' affinity was derived based on four descriptors:

$$K_i(A_1\ AR) = -2.205 * \mathrm{Log}P - 0.087 * E_{steric} + 0.017 * DV_X + 0.027 * SA_{IP+} - 4.218, \quad (1)$$

where Log P is the octanol–water partition coefficient, E_{steric} is the steric energy, DV_X is the X component of the molecule's dipole vector, SA_{IP+} is the positively charged surface area of electrostatic isopotential.

The statistics for the model is shown in Table 4. Regression line obtained by plotting experimental versus predicted K_i values is shown in Figure 5a. The differences between experimental and calculated biological data are presented in Figure 5b. The first descriptor included in Eq. 1 is Log P. Its range is from 1.172 to 5.082 and has a negative sign: an increasing contribution coefficient corresponds to a decrease in K_i value. It reflects the importance of the R^1-alkyl substituents as well as the annelated ring size. The presence of propyl substituents, 6- or 7-membered annelated ring, and phenyl substituent bearing methoxy group or chlorine atom and linked with the tricyclic ring by alkyl chain is advisable. The second descriptor is a steric energy which is the sum of the molecular mechanics potential energies calculated for the bonds, bond angles, dihedral angles, non-bonded atoms, and so forth. Steric energy for the A_1 AR ligands is in the range $-2.549 \div -39.009$ kcal/mol and has

Table 4. Summary of the statistic for A_1AR and A_{2A} AR QSAR models

	Eq. 1	Eq. 2
Number of components	28	65
q^2	0.793	0.817
R^2	0.836	0.841
k	0.836	0.846
k'	1.000	0.998
F	0.646	0.510

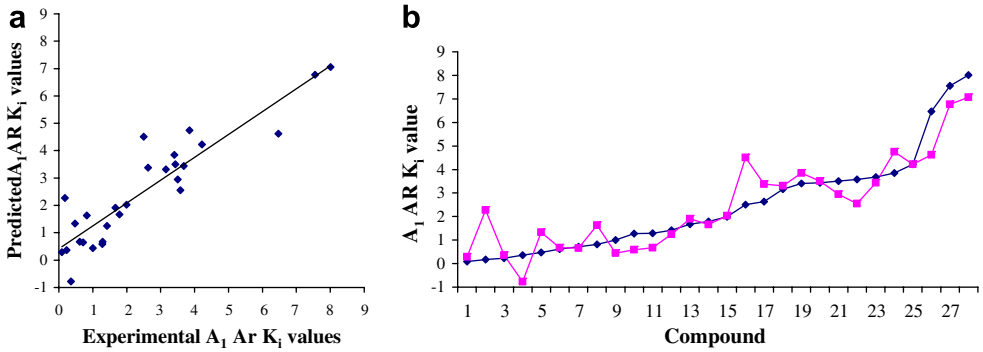

Figure 5. (a) Experimental versus predicted K_i values of A_1 AR binding activity. (b) Comparison of the experimental K_i values (blue, ♦) with those predicted by 3D-QSAR model (rose, ■) for A_1 AR ligands.

negative coefficient in Eq. 1. It is quite sensitive to the size of the substituent, in particular to the linker between the tricyclic ring and phenyl moiety, but the size of annelated ring does slightly affect it. It suggests that the compounds that possess benzyl or phenylalkyl substituents should be preferred to phenyl substituents and long phenylalkyl moieties with the heteroatom in the linker. The third descriptor is the dipole vector—a key electrical property of the molecule, that has both size and direction. It points from the direction of net negative charge to the direction of net positive charge. The best correlation was obtained with the dipole vector X. Its value is from −9.237 to −0.807 and from 0.168 to 7.780 D. This descriptor is affected by the nature of the substituents in the annelated ring. Its direction depends on the linker type. Positive contribution coefficient suggests that for the better affinity to A_1 AR, ligand should possess phenyl ring with small polar substituent or benzyl moiety. The last one descriptor in Eq. 1 is positively charged surface area of electrostatic potential. It is influenced by the substituents in the annelated ring as well as by the R^1-alkyl, although it is not affected by the third ring size. The positive surface area is in the range from 296.479 to 523.067 Å. This descriptor also implies that the electrostatic properties of the substituents in the molecule are important for the A_1 AR binding affinity. It is very sensitive as when changing the position of chlorine atom from *para* to *meta*, it affects not only the purine ring but also R^1 substituents[16] charge distribution (Fig. 6). The presence of the benzyl or phenethyl substituents in the annelated ring bearing halogen atom and long alkyl moiety at R^1 is so suggested.

Three outliers were determined during development of the model which are pyrimidopurinediones with phenyl (**16, 29**)[15] and benzyl (**13**)[16] substituents in the annelated ring. The K_i values for these compounds are 35.0, 19.1, and 17.8 μM, respectively, which is out of K_i range (0.089 ÷ 8.01 μM) for the rest of A_1 AR ligands' database. Such compounds with low micromolar affinity are poorly presented in the sequence in comparison with those possessing submicromolar and micromolar affinities, which may be the reason why the QSAR model is unable to accurately predict their activity.

5.2.2. A_{2A} AR QSAR. Sixty-nine A_{2A} AR ligands (**6**, **7**, **9–12**, **14–19**, **21**, **23–29**, **32**, **34–40**;[15] **1**, **3–10**, **12–20**;[16] **2Aa–i**, **2Ak**, **2Al**, **2Ba–c**, **5b–d**, **6a–d**, **7a**, and **7b**) were collected for the development of 3D-QSAR model. Several QSAR equations were constructed. The model containing the smallest number of the descriptors but leading to the largest increase in q^2 and R^2 was selected as the best one Eq. 2. The following 3D-QSAR equation was derived based on five descriptors:

$$K_i(A_{2A}\,AR) = -0.379 * \mathrm{Log}P + 0.076 * E_{steric} - 0.055 * DV_Y - 0.023 * SA_{IP-} - 0.032 * IF_{ED} + 15.971, \quad (2)$$

where Log P is the octanol–water partition coefficient, E_{steric} is the steric energy, DV_Y is the Y component of the molecule's dipole vector, SA_{IP-} is the negatively charged surface area of electrostatic isopotential, IF_{ED} is the surface integral of electrostatic potential on electron density.

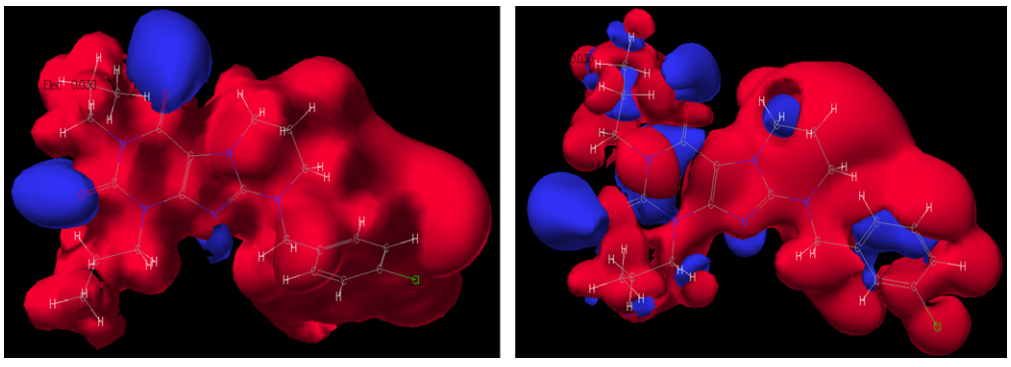

Figure 6. Electrostatic potential isosurface for ligands **16** and **18**[16].

The statistics for the model is shown in Table 4. Regression line obtained by plotting experimental versus predicted A_{2A} AR K_i values is shown in Figure 7a. The differences between experimental and calculated biological data are reported in Figure 7b. The first descriptor included in A_{2A} AR QSAR model is Log *P* and in the range from 0.083 to 5.082. The negative contribution coefficient means that the higher Log *P* value the better A_{2A} AR affinity possessing ligand. The most favorable substituents in the annelated ring are phenethyl and benzyl, bearing chlorine atom or methoxy group, and R^1-propyl moiety. The second descriptor in Eq. 2 is the Y component of the molecule's dipole vector and has negative contribution coefficient that suggests the importance of the vector direction. The dipole moment Y values are is in the range $-7.314 \div -0.020$ and $0.314 \div 4.869$ D. This descriptor affection proposes the preference of phenethyl substituents in the third ring and R^1-methyl groups. The next one descriptor used to derive the Eq. 2 is steric energy which is in the range $-41.423 \div -3.636$ kcal/mol. The nature of annelated ring substituents affects steric energy and as it has positive contribution coefficient, the substituents decreasing its value, such as benzyl and phenethyl along with R^1-methyl groups, are so suggested. The fourth descriptor is a negatively charged surface area of electrostatic potential. It is strongly influenced by the substituents in the annelated ring. The negative surface area is in the range from 103.634 to 278.981 Å. The presence of phenyl substituents bearing methyl or methoxy moiety or phenyl substituents with long alkyl or alkoxyl linker could improve A_{2A} AR K_i value. The last one descriptor in Eq. 2 is surface integral of electrostatic potential on electron density (from 103.126 to 266.291). It is a hybrid shape–property descriptor and represents the surface electronic properties. It encodes the shape of molecular volume and reflects the behavior of the whole molecule which is important when binding to the receptor.

Four outliers were determined which are pyrimidopurinediones with phenyl substituents in the annelated ring (**36**, $K_i = 22.3$ μM)[15] and ligands **5d** ($K_i = 4.6$ μM), **7a** ($K_i = 20.0$ μM), **7b** ($K_i = 14.0$ μM). For compounds **36**, **7a**, and **7d**, the derived QSAR model is unable to accurately predict the K_i values that are out of the data set range (from 0.147 to 8.72 μM) and poorly presented. Instead compound **5d** could be involved in allosteric interactions with the A_{2A}AR.[44] Obviously, for this ligand a change in the mechanism of the reaction occurs at the inversion point.

Comparing obtained A_1 and A_{2A} ARs 3D-QSAR models, it could be noticed that for the A_1 AR binding activity Log *P* has higher importance than for A_{2A} AR affinity as the contribution coefficient is six times higher. Ligands' steric energy has comparable contribution coefficient value but different signs. Different dipole moment vectors, X for A_1 AR and Y for A_{2A} AR, are incorporated in both models. Notably for A_{2A} AR model, the dipole vector affects K_i value three times more than A_1 AR K_i. Moreover, it is significant the opposite directions of these vectors as their contribution coefficients have diverse (positive and negative) meaning. Both QSAR equations incorporate surface area of electrostatic potential. For A_1 AR, this area is positive and has positive contribution coefficient and for the A_{2A} AR model it is negatively charged bearing negative sign. Important that for A_{2A} AR the equation includes information about shape of the molecular volume which suggests that for this AR subtype the surface property is of great importance.

5.3. In vivo tests

Virtually all of the tested compounds were inactive as anticonvulsants; some of the compounds exhibited toxic effects at 0.5 h at scMet test (in the group of arylalkyl derivatives: death following tonic extension after 30 mg/kg of **2Aa**, continuous seizure activity was noticed after 100 mg/kg dose of **2Al**, tonic extension and death following continuous seizure after 300 mg/kg dose of **2Ad**; in the group of carbamates: death following continuous seizure was observed after 100 mg/kg dose of **8c**; death following tonic extension after 300 mg/kg dose of **8d**). Only compounds **2Ah** showed a short time (0.5 h) protection in the MES test at a high dose of 300 mg/kg in mice, and **5c** also exhibited short time (0.5 h) protection in the scMet test in mice at 300 mg/kg (four animals from five tested were protected). At the mice 6 Hz test, ether **5d** has shown some protection at 0.25, 0.5, and 1.0 h time points (one from four animals), and **5b** has shown weaker protection only at 0.25 h (one from four animals).

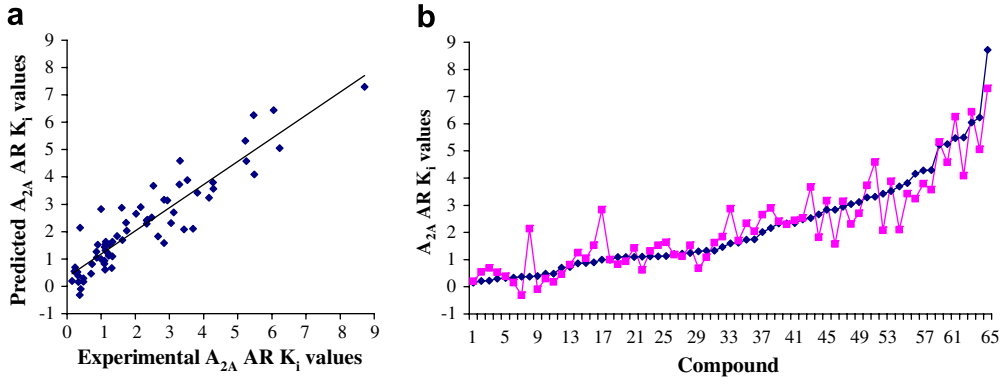

Figure 7. (a) Experimental versus predicted K_i values of A_{2A}AR binding activity. (b) Comparison of the experimental K_i values (blue, ♦) with those predicted by 3D-QSAR model (rose, ■) for A_{2A} AR ligands.

6. Conclusions

In conclusion, we have shown that *N*-phenethyl-substituted pyrimido[2,1-*f*]purinediones and analogs with the modifications of ethylene spacer (substituted or extended) exhibit micromolar or submicromolar affinity for A_{2A} ARs. The kind of substituent at the aromatic ring was important for the affinity. A spacer of two carbon atoms was favorable for high A_{2A} AR affinity. Branched chains as a spacer were more advantageous for A_1 AR affinity. Oxygen and nitrogen atoms in the spacer may result in a slight decrease in A_{2A} and less A_1 ARs affinity. When the 1,3-dimethyl groups were replaced by propyl residues, enhanced affinity for the other AR subtypes was observed, and the A_{2A} selectivity was lost (compare **2Aa** and **2Ba**).

- The best ligands for A_{2A} ARs were compounds **2Ac**, **2Aa**, **2Ak**, and **2Ab**.
- The best ligands for A_1 AR were compounds **2Ba**, **2Bb**, **2Bc**, **7b** (however, with lower selectivity toward A_{2A} AR).

The reliable 3D-QSAR models able to rationalize the activity of A_1 and A_{2A} adenosine receptor for tricyclic xanthine ligands were developed. The analysis of the results depicts that for the A_1 AR binding activity it is important for ligands to possess R^1-bulky substituents along with the phenyl or benzyl substituents bearing halogen atom and phenethyl moiety. For A_{2A} AR affinity it could be favorable to introduce phenethyl or phenyl substituent connected with the tricyclic ring by the alkoxy chain. The nature of R^1 group may not significantly affect the A_{2A} AR affinity.

7. Experimental

7.1. Chemistry general remarks

Melting points were determined on a MEL-TEMP II apparatus and are uncorrected. IR spectra were taken as KBr discs on an FT Jasco IR 410 spectrometer. UV spectra were recorded on Jasco UV–vis V 530 in a concentration of 10^{-4} mol/L in methanol. ^{1}H NMR spectra of compounds **2Ab**, **2Ai**, **2Ae**, and **2Ah** were obtained with a Bruker Ac 200F in $CDCl_3$; compounds **2Ad**, **2Ak** (in $CDCl_3$) and compounds **2Ac** and **5a** (in DMSO-d_6) were analyzed with a Bruker VM250 apparatus; compounds **2Aa**, **2Ag**, **2Aj**, **2Al**, **2Ba**, **2Bc**, **5b**–**d**, and **6a**–**d** were determined with a Varian-Mercury 300 MHz apparatus in $CDCl_3$, and compounds **8a**–**d**, **7a**, and **7b** in DMSO-d_6 using tetramethylsilane as an internal standard. Elemental analyses (CHN) were performed on an Elemental Vario-EL III apparatus and were in accordance with theoretical values within ±0.4%. TLC data were obtained with Merck silica gel $60F_{254}$ aluminum sheets using the following developing systems: (1) benzene/acetone (7:3); (2) toluene/acetone (7:3); (3) toluene/acetone (1:1); (4) CH_2Cl_2/MeOH (18.5:1.5); (5) toluene/acetone/MeOH (5:5:1). Spots were detected under UV light.

7.2. General procedures for the synthesis of 1,3-dialkyl-9-arylalkyl-6,7,8,9-tetrahydropyrimido[2,1-*f*]purine-2,4-(1*H*,3*H*)-diones (Table 2a)

A mixture of 1.65 g (5 mmol) of 7-(3-chloropropyl)-8-bromotheophylline (**1A**) or 0.78 g (2 mmol) of 1,3-dipropyl-7-(3-chloropropyl)-8-bromoxanthine (**1B**) and the appropriate amine (1.4- to 5-fold excess) was refluxed in the appropriate solvent (propanol, butanol, methoxyethanol, DMF) or without solvent (compound **2Ad**) for 5–10 h (see Table 2a). After cooling, a precipitate was formed and was collected by filtration. The precipitate of compound **2Ae**, containing a small amount of unreacted 7-(3-chloropropyl)-8-bromotheophylline, was separated by stirring it with 20% aq HCl solution for 0.5 h, filtered, and reprecipitated by the addition of 10% aq NaOH solution to adjust a pH value of 9. Compounds **2Ba** and **2Bb** were precipitated by adding water to the reaction mixture in DMF.

7.3. General procedure for the synthesis of acetyl derivatives

Acetyl derivatives **2Ah** and **2Ag** were prepared by refluxing of compounds **2Af** and **2Ae** with acetic anhydride for 5 h, removing the excess of anhydride by distillation under reduced pressure and crystallization of the residue.

7.3.1. Synthesis of ether derivatives (Table 2b)

7.3.1.1. 1,3-Dimethyl-9-[2-(4-methylphenoxy)ethyl]-6,7,8,9-tetrahydropyrimido[2,1-*f*]purine-2,4(1*H*,3*H*)-dione (5d). *Method A.* A mixture of 1.02 g (3 mmol) of 1,3-dimethyl-9-bromoethyl-6,7,8,9-tetrahydropyrimido[2,1-*f*]purine-2, 4-(1*H*,3*H*)-dione (**3**)[18] and 0.32 g (3 mmol) of *p*-cresole sodium salt (obtained as in Method C) in 30 mL of dry acetonitrile containing a catalytic amount of [15]-crown-5 was refluxed for 6 h. The mixture was filtered while hot, and the obtained solid contained NaBr. After cooling of the filtrate, product **3** precipitated first, then in the next filtrate the main crop of the product (**5d**) was separated. With the same method, compounds **5b** and **5c** were obtained.

Method B. To a stirred and ice-cold solution of 1.38 g (5 mmol) of 1,3-dimethyl-9-hydroxyethyl-6,7,8,9-tetrahydropyrimido[2,1-*f*]purine-2,4(1*H*,3*H*)-dione (**4**),[19] 1.57 g (6 mmol) of triphenylphosphine, and 0.64 g (6 mmol) of *p*-cresole in 15 mL of dry THF, 0.95 mL (6 mmol) of DEAD (diethyl azodicarboxylate) was added dropwise. Then the reaction mixture was stirred at room temperature overnight. The solvent was removed under reduced pressure, and the obtained oily residue was purified by column chromatography using a mixture of ethyl acetate/chloroform (1:1) as eluent yielding **5d**. With the same method compound **5c** was obtained. For column chromatography separation, first a mixture of ethyl acetate : chloroform (1:1) then chloroform/MeOH (9:1) were used as the eluents.

7.3.1.2. 1,3-Dimethyl-9-(4-chlorophenoxyethyl)-6,7,8,9-tetrahydropyrimido[2,1-*f*]purine-2,4(1*H*,3*H*)-dione (5a). *Method C.* A mixture of 0.34 g (1 mmol) of 1,3-dimethyl-9-bromoethyl-6,7,8,9-tetrahydropyrimido[2,1-*f*]purine-

2, 4-(1*H*,3*H*)-dione (**3**) and 0.3 g (2 mmol) of sodium *p*-chlorophenolate (obtained ex tempore by dissolving *p*-chlorophenol in a hot ethanolic solution of NaOH, subsequently removing the solvent by distillation under reduced pressure and washing the residue with acetone) and 10 mL of methoxyethanol was refluxed for 20 h. After distillation under reduced pressure the residue was washed with water and filtered off.

7.3.1.3. 1,3-Dimethyl-9-[2-(benzyloxy)ethyl]-6,7,8,9-tetrahydropyrimido[2,1-*f*]purine-2,4(1*H*,3*H*)-dione (6a). *Method D.* A suspension of 0.68 g (2.5 mmol) of **4** and 0.12 g (3 mmol) of NaH in dry toluene containing a catalytic amount of [15]-crown-5 was stirred for 24 h at room temperature. Then 0.51 g (3 mmol) of benzyl chloride was added dropwise and the reaction mixture was refluxed for 6 h. The mixture was filtered while hot, and from the cooled filtrate unreacted **4** was separated as a first precipitate. Then the desired product (**6a**) precipitated. With the same method compounds **6b–d** were obtained.

7.3.2. Synthesis of amine derivatives 7a and 7b (Table 2b)

7.3.2.1. Hydrochloride of 1,3-dimethyl-9-[2-(benzylamino)-ethyl]-6,7,8,9-tetrahydropyrimido[2,1-*f*]purine-2,4(1*H*,-3*H*)-dione (7a). *Method E.* Compound **3** 0.85 g (2.5 mmol) and 1.0 g of potassium carbonate were triturated in a mortar and then mixed with 0.27 g (2.5 mmol) of benzylamine. The mixture was melted in a beaker covered with a reversed funnel under microwave irradiation (domestic oven) for 8 min at 450 W. The cooled mixture was extracted with warm methylene chloride. Then the solvent was evaporated and the oily residue was purified by column chromatography using methylene chloride/MeOH (9:1) as an eluent. After evaporation of the eluent under reduced pressure, the residue was dissolved in ethanol and saturated with dry HCl gas. Compound **7b** was obtained with the same method. It was isolated as the free base.

7.3.3. Synthesis of carbamate derivatives (Table 2b)

7.3.3.1. *N*-phenyl carbamate of 1,3-dimethyl-9-(2-hydroxyethyl)-6,7,8,9-tetrahydropyrimido[2,1-*f*]purine-2,4(1*H*,-3*H*)-dione (8a). *Method F.* A mixture of 1.4 g (5 mmol) of **4** and 0.57 g (5 mmol) of phenyl isocyanate in 20 ml of anhydrous acetonitrile was refluxed for 10 h. The resulting solid was filtered off while hot and recrystallized from ethanol.

By the same method compounds **8b–d** were obtained.

The spectral data are summarized in Table 5.

7.4. Pharmacology

7.4.1. Adenosine receptor binding assays. [^{3}H]CCPA (54.9 Ci/mmol) was purchased from NEN Life Sciences; [^{3}H]MSX-2 (85 Ci/mmol), [^{3}H]PSB-11 (53 Ci/mmol), and [^{3}H]PSB-298 (124 Ci/mmol) were obtained from Amersham (custom synthesis). The non-radioactive precursors of [^{3}H]MSX-2 (MSX-1),[25,45] [^{3}H]PSB-11 (PSB-10),[46] and [^{3}H]PSB-298 (PSB-297)[47] were synthesized in our laboratory. [^{3}H]ZM241385 (17 Ci/mmol) was obtained from Tocris. Frozen rat brains obtained from Pel Freez®, Rogers, AR, USA, were dissected to obtain cortical membrane preparations for A_1 assays, and striatal membrane preparations for A_{2A} assays as described.[48] CHO cells recombinantly expressing the human adenosine A_1, A_{2A}, and A_3 receptors were a gift from Dr. K.-N. Klotz, and grown as described.[48,49] Membrane preparations were obtained as previously described.[48,49] For A_{2B} adenosine receptor assays, commercially available membrane preparations containing the human A_{2B} AR were obtained from Biotrend (Cologne, Germany). Stock solutions of the compounds were prepared in dimethylsulfoxide (DMSO), the final concentration of DMSO in the assays did not exceed 2.5%. Initial screening was performed at a single concentration of 25, 10, 2.5, or 1 μM, depending on the solubility of the test compound. Binding assays were performed as previously described.[25,29,47–50] Curves were determined using 6–7 different concentrations of test compounds spanning three orders of magnitude. At least three separate experiments were performed, each in triplicate. For non-linear regression analysis, the Cheng–Prusoff equation and K_D values of 0.2 nM (rat A_1) and 0.6 nM (human A_1), respectively, for [^{3}H]CCPA,[26] 8 nM (rat A_{2A}) and 7 nM (human A_{2A}), respectively, for [^{3}H]MSX-2,[25,51] 33 nM for [^{3}H]ZM241385 (human A_{2B}),[50] 56 nM (human A_{2B}) for [^{3}H]PSB-298 (human A_{2B}),[30] and 4.9 nM (human A_3) for [^{3}H]PSB-11[29] were used to calculate K_i values from IC_{50} values.

7.4.2. Anticonvulsant screening. The preliminary anticonvulsant evaluation was carried out using reported procedures.[30,32,31,33] Male albino mice (F-1 strain, 18–25 g) were used as experimental animals. Groups of 1–5 mice were used in MES, scMet tests, group of 2–8 animals in rotorod test. The tested compounds were suspended in a 0.5% methylcellulose–water mixture. Each compound was administered as an ip injection at three dose levels (30, 100, and 300 mg/kg) with anticonvulsant activity and neurotoxicity assessed at 0.5 and 4 h intervals after administration. Anticonvulsant efficacy was measured by maximal electroshock (MES) and subcutaneous pentylenetetrazole (scMet), neurological deficit was investigated in the rotorod test. Groups of four mice were used in 6 Hz test. Each compound was administered at 100 mg/kg dose, the results were observed after 0.25, 0.5, 1, 2, and 4 h intervals after administration.

7.5. X-ray structure analysis of compound 6d

Crystals of **6d** were obtained by slow evaporation from methanol/ethanol (1:1) solutions. The measurements of the crystals were performed on a Siemens SMART CCD with CuKα radiation ($\lambda = 1.54$Å) at room temperature.

7.6. Crystal data for 6d

$C_{21}H_{25}N_5O_3$, M = 395.46, monoclinic, space group $P2_1/c$ (No.14), $a = 24.563(5)$ Å, $b = 4.7071(9)$ Å, $c = 17.586(4)$ (Å), $\beta = 104.67(3)°$, $V = 1967.0(8)$ Å^3, $Z = 4$, $D_x = 1.335$ g/cm^3, $T = 297$ K, $\mu = 0.749$ mm^{-1}, $\lambda = 1.54178$ Å, $F(000) = 840$, colorless prisms, ($0.1 \times 0.3 \times 0.3$ mm), data/parameters = 3715/375; final $R_1 = 0.043$, $wR_2 = 0.1375$ (all data).

Table 5. Spectral data of the obtained pyrimido[2,1-*f*]purinediones

Compound	IR ν (cm^{-1})	UV λ_{max}, $\log\varepsilon$	^{1}H NMR δ (ppm)
2Aa	3087–3032-phenyl, 2964–2860-CH_2, 1693-CO (pos. 2), 1657-CO (pos. 4), 750-CH_2	299, 4.09	2.02–2.09 (m, 2H, $CH_2CH_2CH_2$), 2.96 (t, J = 7.50 Hz, 2H, CH_2CH_2), 3.21 (t, J = 6.25 Hz, 2H, CH_2CH_2), 3.37 (s, 3H, 3.36 N_3CH_3), 3.52 (s, 3H, N_1CH_3), 3.75 (t, J = 7.50 Hz, 2H, CH_2N_9), 4.17 (t, J = 6.25 Hz, 2H, N_5CH_2), 7.19–7.33 (m, 5H, phenyl)
2Ab	2994–2973-CH_2, 1697-CO (pos. 2), 1656-CO (pos. 4), 1052-OCH_3, 817-phenyl, 748-CH_2	303, 4.30	1.90–2.08 (m, 2H, $CH_2CH_2CH_2$), 2.88 (t, J = 7.00 Hz, 2H, CH_2CH_2), 3.11–3.19 (m, 2H, CH_2CH_2), 3.35 (s, 3H, N_3CH_3), 3.50 (s, 3H, N_1CH_3), 3.67–3.73 (m, 2H, CH_2N_9), 3.78 (s, 3H, OCH_3), 4.14 (t, 2H, J = 6.00 Hz, N_3CH_2), 7.12 (d, 1H, J = 6.60 Hz, 3′-phenyl), 7.28 (d, 1H, J = 4.00 Hz, 5′-phenyl), 7.30–7.36 (m, 2H, 2′6′-phenyl)
2Ac	3382-OH, 3021-phenyl, 2935-CH_2, 1687-CO (pos. 2), 1643-CO (pos. 4), 833-aryl, 750-CH_2	303, 4.09	1.80–2.20 (m, 2H, $CH_2CH_2CH_2$), 2.82 (t, J = 7.20 Hz, 2H, CH_2CH_2), 3.27 (s, 3H, N_3CH_3), 3.31–3.40 (m, 5H, CH_2CH_2 + N_1CH_3), 3.65 (t, J = 7.30 Hz, 2H, CH_2N_9), 4.06 (t, J = 5.70 Hz, 2H, N_5CH_2), 6.73 (d, J = 8.03 Hz, 2H, 3′5′-phenyl, 7.08 (d, J = 8.00 Hz, 2H, 2′6′-phenyl), 9.24 (s, 1H, OH)
2Ad	2938–2844-CH_2, 1695-CO (pos. 2), 1649-CO (pos. 4), 811-phenyl, 748-CH_2	302, 4.29	2.00–2.09 (m, 2H, $CH_2CH_2CH_2$), 2.93 (t, J = 7.75 Hz, 2H, CH_2CH_2), 3.24 (t, J = 5.00 Hz, 2H, CH_2CH_2), 3.35 (s, 3H, N_3CH_3), 3.5 (s, 3H, N_1CH_3), 3.71 (t, J = 8.00 Hz, 2H, CH_2N_9), 4.17 (t, J = 6.00 Hz, 2H, N_5CH_2), 7.13–7.22 (m, 2H, 2′6′-phenyl), 7.23–7.28 (m, 2H, 3′5′-phenyl)
2Ae	3374-OH, 3060–3027-phenyl, 2925–2881-CH_2, 1685-CO (pos. 2), 1645-CO (pos. 4), 833- phenyl, 750-CH_2	302, 4.29	2.01–2.03 (m, 2H, $CH_2CH_2CH_2$), 3.09–3.24 (m, 2H, N_9CH_2), 3.34 (s, 3H, N_3CH_3), 3.50 (s, 3H, N_1CH_3), 3.58–3.64 (m, 1H, CH_2N_9), 3.77–3.98 (m, 1H, CHN_9), 4.14 (t, J = 6.00 Hz, 2H, N_5CH_2), 4.96 (d, J = 4.00 Hz, 1H, OH), 5.04–5.08 (m, 1H, CHOH), 7.27–7.37 (m, 5H, phenyl)
2Af	3316-OH, 3062–3045-phenyl, 2942–2873-CH_2, 1691-CO (pos. 2), 1651-CO (pos. 4), 765-phenyl, 748-CH_2	304, 4.30	1.29 (d, J = 7.20 Hz, 3H, CH_3), 1.6 (s, 1H, OH), 2.02–2.09 (m, 2H, $CH_2CH_2CH_2$), 3.15–3.22 (m, 2H, CH_2N_9), 3.38 (s, 3H, N_3CH_3), 3.54 (s, 3H, N_1CH_3), 4.09–4.20 (m, 2H, N_5CH_2), 5.05–5.07 (m, 1H, $CHCH_3$), 5.30 (d, J = 2.50 Hz, 1H, CHOH), 7.26–7.38 (m, 5H, phenyl)
2Ag	3063–3033-phenyl, 2983–2944-CH_2, 1749-$OCOCH_3$, 1697-CO (pos. 2), 1650-CO (pos. 4), 796-phenyl, 748-CH_2	301, 4.32	1.34 (d, J = 7.10 Hz, 3H, CH_3), 1.86–1.94 (m, 2H, $CH_2CH_2CH_2$), 2.12 (s, 3H, $COCH_3$), 3.11–3.26 (m, 2H, CH_2N_9), 3.36 (s, 3H, N_3CH_3), 3.54 (s, 3H, N_1CH_3), 4.01 (m, 2H, N_5CH_2), 4.69–4.78 (m, 1H, $CHCH_3$), 6.03 (d, J = 6.30 Hz, 1H, $CHOCOCH_3$), 7.24–7.36 (m, 5H, phenyl)
2Ah	3062–3045-phenyl, 2942–2873-CH_2, 1738-$OCOCH_3$, 1703-CO (pos. 2), 1653-CO (pos. 4), 767-phenyl, 744-CH_2		2.01–2.07 (m, 5H, $CH_2CH_2CH_2$ + $COCH_3$), 3.28–3.29 (m, 5H, N_9CH_2 + N_3CH_3), 3.51 (s, 3H, N_1CH_3), 3.83 (d, J = 5.40 Hz, 2H,CH_2N_9), 4.17 (t, J = 6.00 Hz, 2H, N_5CH_2), 6.11 (t, J = 5.60 Hz, 1H, CH), 7.26–7.39 (m, 5H, phenyl)
2Ai	3081-phenyl, 2991–2840-CH_2, 1693-CO (pos. 2), 1655-CO (pos. 4), 1068-OCH_3, 816-phenyl, 750-CH_2	303, 431	1.95–2.05 (m, 2H, $CH_2CH_2CH_2$), 2.88 (t, J = 7.10 Hz, 2H, CH_2CH_2), 3.19 (t, J = 5.60 Hz, 2H, N_9CH_2), 3.34 (s, 3H, N_3CH_3), 3.50 (s, 3H, N_1CH_3), 3.72 (t, J = 7.20 Hz, 2H, CH_2N_9), 3.84 (s, 6H, 2× OCH_3), 4.15 (t, J = 6.00 Hz, 2H, N_5CH_2), 6.73–6.84 (m, 3H, phenyl),
2Aj	3056–3023-pyridyl, 2976–2862-CH_2, 1695-CO (pos. 2), 1662-CO (pos. 4), 743-CH_2	305, 4.32	2.00–2.09 (m, 2H, $CH_2CH_2CH_2$), 3.14 (t, J = 7.51 Hz, 2H, CH_2CH_2), 3.28 (t, J = 6.26 Hz, 2H, N_9CH_2), 3.36 (s, 3H, N_3CH_3), 3.51 (s, 3H, N_1CH_3), 3.92 (t, J = 6.25 Hz, 2H, CH_2N_9), 4.23 (t, J = 5.00 Hz, 2H, N_5CH_2), 7.15–7.19 (m, 2H, 3′5′-pyridyl), 7.57–7.61 (m, 1H, 4′-pyridyl), 8.52–8.54 (m, 1H, 6′-pyridyl)
2Ak	3322-NH, 3106–3058-phenyl, 2973–2842-CH_2, 1697-CO (pos. 2), 1649-CO (pos. 4), 817-phenyl, 740-CH_2		2.06–2.15 (m, 2H, $CH_2CH_2CH_2$), 3.19 (t, J = 7.40 Hz, 2H, CH_2CH_2), 3.28 (t, J = 5.60 Hz, 2H, N_9CH_2), 3.46 (s, 3H, N_3CH_3), 3.62 (s, 3H, N_1CH_3), 3.93 (t, J = 7.40 Hz, 2H, CH_2N_9), 4.24 (t, J = 6.00 Hz, 2H, N_5CH_2), 7.07–7.32 (m, 4H, phenyl), 7.75–7.80 (m, 1H, 2′-pirol)
2Al	3057–3023-phenyl, 2976–2863-CH_2, 1695-CO (pos. 2), 1662-CO (pos. 4), 793-CH_2	301, 4.29	1.92–2.04 (m, 2H, $CH_2CH_2CH_2$), 2.05–2.14 (m, 2H, $CH_2CH_2CH_2$), 2.68 (t, J = 7.50 Hz, 2H, $CH_2CH_2CH_2$), 3.31 (t, J = 6.30 Hz, 2H, N_9CH_2), 3.37 (s, 3H, N_3CH_3), 3.50–3.60 (m, 5H, N_1CH_3 + CH_2N_9), 4.18 (t, J = 6.30 Hz, 2H, N_5CH_2), 7.16–7.31 (m, 5H, phenyl)

Table 5 (*continued*)

Compound	IR ν (cm^{-1})	UV λ_{max}, log ε	^{1}H NMR δ (ppm)
2Ba	3081–3001-phenyl, 2962–2859-CH_2, 1697-CO (pos. 2), 1651-CO (pos. 4), 753-phenyl, 707-CH_2	303.5, 4.28	0.92–1.00 (m, 6H, 2 C*H*$_3$CH$_2$CH$_2$), 1.61–1.85 (m, 4H, 2 CH$_3$C*H*$_2$CH$_2$), 2.00–2.08 (m, 2H, CH$_2$C*H*$_2$CH$_2$), 2.95 (t, *J* = 7.30 Hz, 2H, CH$_2$C*H*$_2$), 3.21 (t, *J* = 5.60 Hz, 2H, N$_9$CH$_2$), 3.74 (t, *J* = 7.30 Hz, 2H, CH$_2$N$_9$), 3.91–4.04 (2 x m, 4H, N$_1$,N$_3$-C*H*$_2$CH$_2$CH$_3$), 4.17 (t, *J* = 6.10 Hz, 2H, N$_5$CH$_2$), 7.20–7.30 (m, 5H, phenyl)
2Bb	3058-phenyl, 2958–2832-CH_2, 1699-CO (pos. 2), 1653-CO (pos. 4), 1261-CH_3O-phenyl, 1028-CH_3O-phenyl, 819-phenyl, 755-CH_2	302, 4.32	0.92–0.99 (m, 6H, 2 × C*H*$_3$CH$_2$CH$_2$), 1.60–1.85 (m, 4H, 2 × CH$_3$C*H*$_2$CH$_2$), 2.01–2.08 (m, 2H, C*H*$_2$CH$_2$CH$_2$), 2.89 (t, *J* = 7.30 Hz, 2H, N$_9$CH$_2$), 3.21 (t, *J* = 6.00 Hz, 2H, CH$_2$N$_9$), 3.71 (t, *J* = 7.30 Hz, CH$_2$C*H*$_2$), 3.86 (s, 6H, 2 × OCH$_3$), 3.90–3.99 (m, 4H, N$_1$, N$_3$C*H*$_2$CH$_2$CH$_3$), 4,17 (t, *J* = 5.90 Hz, 2H, N$_5$CH$_2$),6.72–6.81 (m, 3H, phenyl)
2Bc	3290-NH, 3061–3011-phenyl, 2958–2873-CH_2, 1693-CO (pos. 2), 1650-CO (pos. 4), 756-phenyl, 740-CH_2	302.5, 4.26	0.93–1.02 (m, 6H, 2× C*H*$_3$CH$_2$CH$_2$), 1.61–1.88 (m, 4H, 2× CH$_3$C*H*$_2$CH$_2$), 2.01–2.09 (m, 2H, CH$_2$C*H*$_2$CH$_2$), 3.11 (t, *J* = 7.40 Hz, 2H, CH$_2$C*H*$_2$), 3.29 (t, *J* = 5.60 Hz, 2H, N$_9$CH$_2$), 3.82 (t, *J* = 7.60 Hz, 2H, CH$_2$N$_9$), 3.93–4.08 (m, 4H, N$_1$, N$_3$-C*H*$_2$CH$_2$CH$_3$), 4.18 (t, *J* = 5.90 Hz, 2H, N$_5$CH$_2$), 7.03–7.39 (m, 4H, phenyl), 7.74 (d, *J* = 8.90 Hz, 1H, 2′-pirol), 8.15 (s, 1H, NH)
5a	2985–2883-CH_2, 1697-CO (pos. 2), 1657-CO (pos. 4), 1043-aryl-O, 823-phenyl, 752-CH_2	300.6, 4.27	2.01–2.05 (m, 2H, CH$_2$C*H*$_2$CH$_2$), 3.22 (s, 3H, N$_3$CH$_3$), 3.32 (s, 3H, N$_1$CH$_3$), 3.48 (t, *J* = 5.00 Hz, 2H, CH$_2$O), 3.81 (t, *J* = 6.00 Hz, 2H, N$_9$CH$_2$), 4.05 (t, *J* = 6.30 Hz, 2H, CH$_2$N$_9$), 4.20 (t, *J* = 6.30 Hz, 2H, N$_5$CH$_2$), 6.95–7.01 (m, 2H, 2′6′-phenyl), 7.27–7.33 (m, 2H, 3′5′-phenyl)
5b	3095-phenyl, 2942, 2881-CH_2, 1698-CO (pos. 2), 1654-CO (pos. 4), 1042 (aryl-O-), 8.09-phenyl, 750-CH_2	298.5, 4.59	2.12–2.26 (m, 2H, CH$_2$C*H*$_2$CH$_2$), 3.35 (s, 3H, N$_3$CH$_3$), 3.48 (s, 3H, N$_1$CH$_3$), 3.67 (t, *J* = 5.60 Hz, 2H, N$_9$CH$_2$), 3.93 (t, *J* = 4.82 Hz, 2H, CH$_2$N$_9$), 4.19–4.26 (m, 4H, N$_5$CH$_2$CH$_2$O), 6.84 (d, *J* = 8.80 Hz, 1H, 6′-phenyl), 7.16 (dd, *J* = 6.32 Hz, *J* = 2.47 Hz, 1H, 5′-phenyl), 7.35 (d, *J* = 2.47 Hz, 1H, 3′-phenyl)
5c	3135-NH, 3080-phenyl, 2927-CH_2, 1699-CO (pos. 2), 1653-CO (pos. 4), 1045 (aryl-O-), 831-phenyl, 745-CH_2	4.60	2.08–2.20 (m, 5H, CH$_2$C*H*$_2$CH$_2$ + CH$_3$CO), 3.35 (s, 3H, N$_3$CH$_3$), 3.46–3.57 (m, 5H, N$_1$CH$_3$ + N$_9$CH$_2$), 3.87 (t, *J* = 5.13 Hz, 2H, CH$_2$N$_9$), 4.17–4.24 (m, 4H, N$_5$CH$_2$, CH$_2$O), 6.83 (d, *J* = 8.79 Hz, 2H, 3′5′-phenyl), 7.26 (s, 1H, NHCO), 7.37 (d, *J* = 8.40 Hz, 2H, 2′,6′-phenyl)
5d	3032-phenyl, 2930, 2877-CH_2, 1702-CO (pos. 2), 1658-CO (pos. 4), 1045 (aryl-O-), 813-phenyl, 755-CH_2	297.5	2.02–2.20 (m, 2H, CH$_2$C*H*$_2$CH$_2$), 2.27 (s, 3H, CH$_3$), 3.35 (s, 3H, N$_3$CH$_3$), 3.49 (s, 3H, N$_1$CH$_3$), 3.57 (t, *J* = 5.50 Hz, 2H, CH$_2$O), 3.88 (t, *J* = 5.13 Hz, 2H, N$_9$CH$_2$), 4.18 (m, 4H, N$_9$CH$_2$, CH$_2$N$_9$), 6.78 (d, *J* = 8.40 Hz, 2H, 2′,6′-phenyl), 7.06 (d, *J* = 8.52 Hz, 2H, 3′,5′-phenyl)
6a	3066, 3033-phenyl, 2940, 2909, 2885-CH_2, 1698-CO (pos. 2), 1651-CO (pos.4), 1042 (aryl CH_2O), 819-phenyl, 741-CH_2		2.10 (q, *J* = 5.77 Hz, 2H, CH$_2$C*H*$_2$CH$_2$), 3.36 (s, 3H, N$_3$CH$_3$), 3.44–3.50 (m, 5H, N$_1$CH$_3$ + CH$_2$O), 3.72 (s, 4H, CH$_2$N$_9$, N$_9$CH$_2$), 4.19 (t, *J* = 5.90 Hz, 2H, N$_5$CH$_2$), 4.52 (s, 2H, C*H*$_2$-phenyl), 7.25–7.34 (m, 5H, phenyl)
6b	3055-phenyl, 2936, 2870–CH_2, 1698-CO (pos. 2), 1653-CO (pos.4), 1043 (aryl CH_2O), 844-phenyl, 742-CH_2	295.5, 4.56	2.11 (q, *J* = 5.20 Hz, 2H, CH$_2$C*H*$_2$CH$_2$), 3.35 (s, 3H, N$_3$CH$_3$), 3.47–3.52 (m, 5H, N$_1$CH$_3$ + CH$_2$O), 3.71 (s, 4H, CH$_2$N$_9$, N$_9$CH$_2$), 4.20 (t, *J* = 6.05 Hz, 2H, N$_5$CH$_2$), 4.48 (s, 2H, CH$_2$-phenyl), 7.19–7.30 (m, 4H, phenyl)
6c	3055-phenyl, 2923, 2852-CH_2, 1698-CO (pos. 2), 1653-CO (pos. 4), 1045 (aryl CH_2O-), 825-phenyl, 7.42-CH_2	298.5, 4.58	2.10 (q, *J* = 5.77 Hz, 2H, CH$_2$C*H*$_2$CH$_2$), 3.35 (s, 3H, N$_3$CH$_3$), 3.46–3.50 (m, 5H, N$_1$CH$_3$ + CH$_2$O), 3.71 (s, 4H, CH$_2$N$_9$, N$_9$CH$_2$), 4.19 (t, *J* = 6.05 Hz, 2H, N$_5$CH$_2$), 4.47 (s, 2H, CH$_2$ phenyl), 6.97–7.03 (m, 2H, 3′,5′-phenyl), 7.22–7.27 (m, 2H, 2′,6′-phenyl)
6d	3079, 3055, 3025-phenyl, 2938, 2872, 2836, 2803-CH_2, 1696-CO (pos. 2), 1659-CO (pos. 4), 999 (aryl CH_2O), 749-CH_2	302.5, 4.58, 251, 4.50	2.13 (q, *J* = 5.70 Hz, 2H, CH$_2$C*H*$_2$CH$_2$), 3.35 (s, 3H, N$_3$CH$_3$), 3.46–3.53 (m, 5H, N$_1$CH$_3$ + CH$_2$O), 3.72 (s, 4H, CH$_2$N$_9$, N$_9$CH$_2$), 4.14–4.22 (m, 2H, N$_5$CH$_2$), 6.18–6.27 (m, 1H, CH═), 6.55 (d, *J* = 15.95 Hz, 1H, aryl C*H*═), 7.23–7.35 (m, 5H, phenyl)
7a	2950-CH_2, 1699-CO (pos. 2), 1654-CO (pos. 4), 881-phenyl, 748-CH_2	300.0, 4.70	2.06–2.10 (m, 2H, CH$_2$C*H*$_2$CH$_2$), 3.14 (s, 3H, N$_3$CH$_3$), 3.29 (s, 3H, N$_1$CH$_3$), 3.14–3.21 (m, 2H, C*H*$_2$NH), 3.34 (t, *J* = 7.40 Hz, 2H, CH$_2$N$_9$), 3.73 (t, *J* = 6.05 Hz, 2H, N$_9$CH$_2$), 4.03 (t, *J* = 5.91 Hz, 2H, NHC*H*$_2$), 4.19 (t, *J* = 5.64 Hz, 2H, N$_5$CH$_2$), 7.38–7.43 (m, 3H, 3′,4’,5′-phenyl), 7.45–7.56 (m, 2H, 2′,6′-phenyl), 9.48 (s, 2H, NH_2^+)

(*continued on next page*)

Table 5 (*continued*)

Compound	IR ν (cm^{-1})	UV λ_{max}, log ε	^{1}H NMR δ (ppm)
7b	3043-phenyl, 2822-CH_2, 1697-CO (pos. 2), 1644-CO (pos. 4), 837-phenyl, 750-CH_2	300.0, 4.70	1.99–2.04 (m, 2H, $CH_2CH_2CH_2$), 2.69 (t, J = 6.33 Hz, 2H, CH_2NH), 3.14 (s, 3H, N_3CH_3), 3.29 (s, 3H, N_1CH_3), 3.36 (t, J = 5.64 Hz, 2H, CH_2N_9), 3.52 (t, J = 6.33 Hz, 2H, N_9CH_2), 3.67 (s, 2H, $NHCH_2$), 4.03 (t, J = 6.05 Hz, 2H, N_5CH_2), 7.04–7.10 (m, 2H, 3′,5′-phenyl), 7.28–7.33 (m, 2H, 2′,6′-phenyl)
8a	3289-NH, 3076-phenyl, 2949-CH_2, 1727-CONH, 1698-CO (pos. 2), 1650-CO (pos. 4), 1068-CH_2O, 849-phenyl, 759-CH_2	300.0, 5.20	2.03–2.07 (m, 2H, $CH_2CH_2CH_2$), 3.11 (s, 3H, N_3CH_3), 3.18 (s, 3H, N_1CH_3), 3.44 (t, J = 5.50 Hz, 2H, CH_2N_9), 3.74 (t, J = 5.23 Hz, 2H, N_9CH_2), 4.03 (t, J = 5.91 Hz, 2H, N_5CH_2), 4.29 (t, J = 5.23 Hz, 2H, CH_2O), 6.91–6.96 (m, 1H, 4'-phenyl), 7.20 (d, J = 7.98 Hz, 2H, 3′,5′-phenyl), 7.37 (d, J = 7.43 Hz, 2H, 2′,6′-phenyl), 9.52 (s, 1H, NH)
8b	3289-NH, 3083-phenyl, 2943-CH_2, 1733-CONH, 1696-CO (pos. 2), 1640-CO (pos. 4), 1064-CH_2O, 748-CH_2	300.0, 4.60	2.03–2.07 (m, 2H, $CH_2CH_2CH_2$), 3.11 (s, 3H, N_3CH_3), 3.17 (s, 3H, N_1CH_3), 3.43 (t, J = 5.36 Hz, 2H, CH_2N_9), 3.75 (t, J = 4.96 Hz, 2H, N_9H_2), 4.03 (t, J = 5.78 Hz, 2H, N_5CH_2), 4.31 (t, J = 5.01 Hz, 2H, CH_2O), 6.97–6.99 (m, 1H, 5′-phenyl), 7.25 (m, 2H, 4′,6′-phenyl), 7.49 (s, 1H, 2′-phenyl), 9.74 (s, 1H, NH)
8c	3300-NH, 3071-phenyl, 2939-CH_2, 1731-CONH, 1695-CO (pos. 2), 1646-CO (pos. 4), 1074-CH_2O, 841-phenyl, 749-CH_2	300.0, 4.80	2.03–2.06 (m, 2H, $CH_2CH_2CH_2$), 3.11 (s, 3H, N_3CH_3), 3.18 (s, 3H, N_1CH_3), 3.43 (t, J = 5.37 Hz, 2H, CH_2N_9), 3.73 (t, J = 5.01 Hz, 2H, N_9CH_2), 4.03 (t, J = 5.78 Hz, 2H, N_5CH_2), 4.28 (t, J = 5.09 Hz, 2H, CH_2O), 7.05 (t, J = 8.80 Hz, 2H, 3′,5′-phenyl, 7.37 (br s, 2H, 2′,6′-phenyl), 9.58 (s, 1H, NH)
8d	3299-NH, 2939-CH_2, 1735-CONH, 1698-CO (pos.2), 1638-CO (pos. 4), 1088-CH_2O, 750-CH_2	300.0, 4.60	2.03–2.07 (m, 2H, $CH_2CH_2CH_2$), 3.11 (s, 3H, N_3CH_3), 3.17 (s, 3H, N_1CH_3), 3.42–3.45 (m, 2H, CH_2N_9), 3.74 (t, J = 4.98 Hz, 2H, N_9CH_2), 4.03 (t, J = 5.78 Hz, 2H, N_5CH_2), 4.29 (t, J = 4.95 Hz, 2H, CH_2O), 7.25 (d, J = 8.80 Hz, 2H, 3′,5′-phenyl), 7.38 (d, J = 7.43 Hz, 2H, 2′,6′-phenyl), 9.68 (s, 1H, NH)

The structure was solved by a direct method using the SHELXTS program[52] and refined with the SHELXTL.[53] E-map provided positions for all non-H-atoms. The full-matrix least-squares refinement was carried out on F^2s using anisotropic temperature factors for all non-H-atoms. The H-atoms were located from $\Delta\rho$-map, then the positions of H-atoms were refined in the riding model with isotropic thermal parameters. Crystallographic data (excluding structural factors) for the structure reported in this paper have been deposited with the Cambridge Crystallographic Data Centre and allocated the deposition number: CCDC 628859. Copies of the data can be obtained free of charge on application to CCDC, 12 Union Road, Cambridge CB2 1EW, UK (fax: +(1223)336-033; E-mail:deposit@ccdc.cam.ac.uk).

7.7. Computational procedures

For all calculations CAChe 6.1.1[37] software was used. The starting models of the molecules were based on crystallographic data for **6d** using the PCMODEL 6 program.[54] The structures of the synthesized compounds

Table 6. Molecular descriptors and methods for their calculation

Descriptor	Method of calculation
Log P; Molar refractivity	Atom typing scheme of Ghose and Crippen
Connectivity indexes 0–2; Valence connectivity indexes 0–2	Calculated from the chemical sample atoms and bonds
Single, double bonds; Carbon, Oxygen atoms	Extracted from the chemical sample
Shape index order 1–3	Determined by the topological structure of the chemical sample
Solvent accessible surface area; dielectric energy	Calculated at the molecule geometry in water from optimization using MOPAC with PM5 parameters and the Conductor like Screening Model (COSMO)
Dipole moment; Dipole vectors X, Y, Z	Calculated by DFT using D-VWN LDA functional with DZVP basis set at current geometry
Polarizability; HOMO, LUMO energies	Calculated by DFT using the B88-LYP GGA energy functional with the 6-31G** basis sets
Steric energy	Determined by mechanics using augmented MM3
Surface integral of electrostatic isopotential; surface area	Generated by a Dgauss/DFT wave function using the B88-LYP GGA functional with the 6-31G** basis sets
Surface integral of electrostatic potential on electron density; surface area	Calculated by a Dgauss/DFT wave function using the B88-LYP GGA functional with the 6-31G** basis sets
Surface integral of electrostatic potential on van der Waals surface; surface area	Calculated by a DGauss/DFT wave function using the B88-LYP GGA functional with the 6-31G** basis sets

were built and geometry was optimized in MOPAC (Molecular Orbital Package) using semi-empirical Hamiltonian to minimize the energy. To find the low-energy conformers, CONFLEX application was used. The energy of each conformation was plotted in a three-dimensional graph. The low-energy conformations, separated by high energy barriers, were collected and optimized using DFT methods B88-LYP functional with 6-31G** basis set. The descriptors were calculated in CAChe 6.1.1[37] (Table 6).

Acknowledgments

The authors are grateful to Professor James Stables for providing the biological data through the ADD Program of the National Institute of Neurological and Communicative Disorders and Stroke at the National Institutes of Health, Bethesda, MD, USA. We thank Professor Dr. K.-N. Klotz, University of Würzburg, for the gift of recombinant CHO cells expressing adenosine receptor subtypes. This work was supported by Polish State Committee for Scientific Research (Grant No. 6 P05F 024 21) and by the Deutsche Forschungsgemeinschaft (GRK 677).

Supplementary data

Supplementary data associated with this article can be found, in the online version, at doi:10.1016/j.bmc.2007.07.051.

References and notes

1. Fredholm, B. B.; IJzerman, A. P.; Jacobson, K. A.; Klotz, K.-N.; Linden, J. *Pharmacol. Rev.* **2001**, *53*, 527.
2. Ralevic, V.; Burnstock, G. *Pharmacol. Rev.* **1998**, 50.
3. Müller, C. E. *Curr. Med. Chem.* **2000**, *7*, 1269.
4. Dhalla, A. K.; Shryock, J. C.; Shreeniwas, R.; Bellardinelli, L. *Curr. Top. Med. Chem.* **2003**, *3*, 369.
5. Poulsen, S.-A.; Quinn, R. J. *Bioorg. Med. Chem.* **1998**, *6*, 619.
6. Müller, C. E. *Exp. Opin. Ther. Patents* **1997**, *7*, 419.
7. Hess, S. *Exp. Opin. Ther. Patents* **2001**, *11*, 1533.
8. Yuzlenko, O.; Kieć-Kononowicz, K. *Curr. Med. Chem.* **2006**, *13*, 3609.
9. Müller, C. E. *Drugs Future* **2000**, *25*, 1043.
10. Baraldi, P. G.; Tabrizi, M. A.; Bovero, A.; Avitabile, B.; Preti, D.; Fruttarolo, F.; Romagnoli, R.; Varani, K.; Borea, P. A. *Eur. J. Med. Chem.* **2003**, *38*, 367.
11. Rockitt, S.; Duddeck, H.; Drabczyńska, A.; Kieć-Kononowicz, K. *Eur. J. Org. Chem.* **2000**, 3489.
12. Kieć-Kononowicz, K.; Drabczyńska, A.; Pękala, E.; Michalak, B.; Müller, C. E.; Schumacher, B.; Karolak-Wojciechowska, J.; Duddeck, H.; Rockitt, S.; Wartchow, R. *Pure Appl. Chem.* **2001**, *73*, 1411.
13. Drabczyńska, A.; Schumacher, B.; Müller, C. E.; Karolak-Wojciechowska, J.; Michalak, B.; Pękala, E.; Kieć-Kononowicz, K. *Eur. J. Med. Chem.* **2003**, *38*, 397.
14. Drabczyńska, A.; Müller, C. E.; Schumacher, B.; Hinz, S.; Karolak-Wojciechowska, J.; Michalak, B.; Pękala, E.; Kieć-Kononowicz, K. *Bioorg. Med. Chem.* **2004**, *12*, 4895.
15. Drabczyńska, A.; Müller, C. E.; Lacher, S. K.; Schumacher, B.; Karolak-Wojciechowska, J.; Nasal, A.; Kawczak, P.; Yuzlenko, O.; Pękala, E.; Kieć-Kononowicz, K. *Bioorg. Med. Chem.* **2006**, *14*, 7258.
16. Drabczyńska, A.; Müller, C. E.; Karolak-Wojciechowska, J.; Schumacher, B.; Schiedel, A.; Yuzlenko, O.; Kieć-Kononowicz, K. *Bioorg. Med. Chem.* **2007**, *15*, 5003.
17. Rockitt, S.; Wartchow, R.; Duddeck, H.; Drabczyńska, A.; Kieć-Kononowicz, K. *Z. Naturforsch.* **2001**, *56b*, 319.
18. Pawłowski, M.; Drabczyńska, A.; Gorczyca, M.; Malec, D.; Modzelewski, J. *Pol. J. Pharm.* **1991**, *43*, 61.
19. Eckstein, M. *Dissert. Pharm.* **1962**, *14*, 435.
20. Mitsunobu, O. *Synthesis* **1981**, 1.
21. El-Shaieb, K. M. *Heteroat. Chem.* **2006**, *17*, 365.
22. McCarroll, A. J.; Sandham, D. A.; Titcomb, L. R.; de K. Lewis, A. K.; Cloke, F. G. N.; Davies, B. P.; Perez de Santana, A.; Hiller, W.; Caddick, S. *Mol. Divers.* **2003**, *7*, 115.
23. Bergmann, F.; Dikstein, S. *J. Am. Chem. Soc.* **1955**, *77*, 691.
24. Rybár, A.; Antoš, K. *Collect. Czech. Chem. Commun.* **1970**, *35*, 1415.
25. Müller, C. E.; Maurinsh, J.; Sauer, R. *Eur. J. Pharm. Sci.* **2000**, *10*, 259.
26. Klotz, K.-N.; Lohse, M. J.; Schwabe, U.; Cristalli, G.; Vittori, S.; Grifantini, M. *Naunyn Schmiedeberg's Arch. Pharmacol.* **1989**, *340*, 679.
27. Ji, X.-D.; Jacobson, K. A. *Drug Des. Discov.* **1999**, *16*, 217.
28. Yan, L.; Müller, C. E. *J. Med. Chem.* **2004**, *47*, 1031.
29. Yan, L.; Bertarelli, D. C. G.; Hayallah, A. M.; Meyer, H.; Klotz, K.-N.; Müller, C. E. *J. Med. Chem.* **2006**, *49*, 4384.
30. Müller, C. E.; Diekmann, M.; Thorand, M.; Ozola, V. *Bioorg. Med. Chem. Lett.* **2002**, *12*, 501.
31. Porter, R. J.; Cereghino, J. J.; Gladding, G. D.; Kupferberg, H. J.; Scoville, B.; White, B. G. *Clev. Clin.* **1984**, *51*, 293.
32. Krall, R. L.; Penry, J. K.; White, B. G.; Kupferberg, H. J.; Swinyard, E. A. *Epilepsia* **1978**, *19*, 409.
33. Stables, J. P.; Kupferberg, K. J. In *Molecular and Cellular Targets for Antiepileptic Drugs*; John Libbey: London, 1998; pp 191–198.
34. Barton, M. E.; Klein, B. D.; Wolf, H. H.; White, S. *Epilepsy Res.* **2001**, *47*, 217.
35. Kaminski, R. M.; Livingood, M. R.; Rogawski, M. R. *Epilepsia* **2004**, *45*, 864.
36. Gao, Z. G.; IJzerman, A. P. *Biochem. Pharmacol.* **2000**, *60*, 669.
37. CAChe, Version 6.1.1. Sunnyvale, Fujitsu Computer Systems, 2002.
38. Hawkins, D. M.; Basak, S. C.; Mills, D. *J. Chem. Inf. Comput. Sci.* **2003**, *43*, 579.
39. Golbraikh, A.; Shen, M.; Xiao, Z.; De Xiao, Y.; Lee, K.-H.; Tropsha, A. *J. Comp. Aided Mol. Des.* **2003**, *17*, 241.
40. Golbraikh, A.; Tropsha, A. *J. Mol. Graphics Modell.* **2002**, *20*, 269.
41. Hawkins, D. M. *J. Chem. Inf. Comput. Sci.* **2004**, *44*, 1.
42. Cronin, M. T.; Schultz, T. W. *THEOCHEM* **2003**, *622*, 39.
43. He, L.; Jurs, P. C. *J. Mol. Graphics Modell.* **2005**, *23*, 503.
44. Verma, R. P.; Hansch, C. *Bioorg. Med. Chem.* **2005**, *13*, 4597.
45. Hockemeyer, J.; Burbiel, J. C.; Müller, C. E. *J. Org. Chem.* **2004**, *69*, 3308.
46. Burbiel, J.; Thorand, M.; Müller, C. E. *Heterocycles* **2003**, *60*, 1425.
47. Bertarelli, D. C. G.; Diekmann, M.; Hayallah, A. M.; Rüsing, D.; Iqbal, J.; Preiss, B.; Verspohl, E. J.; Müller, C. E. *Purinergic Signalling*, in press.

48. Bulicz, J.; Bertarelli, D. C. G.; Baumert, D.; Fülle, F.; Müller, C. E.; Heber, D. *Bioorg. Med. Chem.* **2006**, *14*, 2837.
49. Klotz, K.-N.; Hessling, J.; Hegler, J.; Owman, C.; Kull, B.; Fredholm, B. B.; Lohse, M. J. *Naunyn Schmiedeberg's Arch. Pharmacol.* **1998**, *357*, 1.
50. Hayallah, A. M.; Sandoval-Ramírez, J.; Reith, U.; Schobert, U.; Preiss, B.; Schumacher, B.; Daly, J. W.; Müller, C. E. *J. Med. Chem.* **2002**, *45*, 1500.
51. Sauer, R.; Maurinsh, J.; Reith, U.; Fülle, F.; Klotz, K.-N.; Müller, C. E. *J. Med. Chem.* **2000**, *43*, 440.
52. Sheldrick, G. M. SHELXTL PC^{MT}, Siemens Analytical X-Ray Instruments Inc., Madison, Wisconsin, USA, **1990**.
53. Sheldrick G. M. SHELXL-97.A FORTRAN-77 Program for the Refinement of Crystal Structures from Diffraction Data. University of Göttingen, Germany, **1997**.
54. PCMODEL 6 Molecular Modeling Software for the IBM PC, Serena Software, Bloomington; 1996.